POLITECNICO DI MILANO

School of Industrial and Information Engineering

Master of Science in Materials Engineering and Nanotechnology

Fracture and Cracking Phenomena in Thin Films.
The Pulsed Laser Deposition Alumina coating case study

Advisor:
Prof. M. G. Beghi

Candidate:
Davide Meroni
925676

Academic Year 2021/2022

Abstract

Thin films are the most prominent coating technology for protection against corrosive environments, in particular this work will analyse the case study of alumina thin films deposited by pulsed laser deposition, which is a good candidate for protection of generation IV nuclear reactors, based on austenitic steel, against coolant materials.

One critical issue is related to the adhesion of such material on stainless steel substrate, and in particular the importance of finding a suitable measurement technique able to quantitatively define some experimental results related to adhesion. There are several methods exploiting adhesion, however, each of them is affected by some limitations. The present work illustrates one of the most promising techniques, based on the uniaxial tensile testing. This method relies on the observation by SEM of the crack formation and evolution within the coating. This peculiar feature of the tensile test is useful to extrapolate not only mechanical properties of the coating, such as fracture toughness, but also adhesion properties, like fracture resistance of the interface and the interfacial shear strength.

In order to extrapolate important results from this technique, it is crucial to understand the principle of coating fracture by uniaxial tensile stresses, thus, an exhaustive illustration of this phenomenon is supported by a deep theory revision. SEM images are provided courtesy by Polytechnique of Turin, and approximate results can be extrapolated, however, a more detailed analysis has to be carried out to assess how the different properties change as a function of the coating thicknesses, taking into account other factors like residual stresses. Moreover, a simulation with appropriate finite element analysis can deepen further the results' meaning.

Keywords: Coating fracture, Interfaces, Fracture toughness, Alumina, Thin film, Adhesion

Estratto in lingua italiana

L'evoluzione tecnologica è stata fin dai tempi antichi una continua sfida per l'essere umano, il quale è sempre stato indotto a sviluppare nuove strategie a seconda delle condizioni e dell'epoca in cui viveva. La continua ricerca di materiali sin dai tempi antichi ha da sempre rappresentato uno dei fattori cardine per lo sviluppo e il benessere della società. Si è passati da una selezione estremamente limitata di materiali nelle epoche più antiche fino ad oggi dove la scoperta della struttura atomica che compone i diversi materiali è tuttora oggetto di studio per realizzare nuovi materiali, con proprietà sempre più performanti.

La scoperta della struttura atomica dei materiali è stata la pietra miliare negli ultimi decenni, poiché la conoscenza approfondita della materia ha portato ad una maggiore processabilità il materiale stesso in differenti ambiti, uno di questi riguarda la possibilità di produrre film sottili. Seppur con tante limitazioni, questa idea era ben nota nella storia. L'uomo aveva bisogno di proteggere i propri manufatti dall'ambiente esterno oppure di decorare statue e cimeli, da qui era cruciale l'importanza di trovare metodi per poter far aderire un materiale completamente differente da quello da proteggere. La complessità di questa operazione ad ogni modo è stata sempre compensata con il progresso tecnologico fino a rendere l'utilizzo di rivestimenti superficiali indispensabile in molti ambiti diversificati, dall'energetica all'elettronica, passando all'ambito del nucleare. Una delle applicazioni che più ha impattato tecnologicamente è l'utilizzo di rivestimenti anticorrosione in ambito civile ed industriale.

Per garantire l'efficacia di questi rivestimenti, l'adesione di un materiale rispetto ad un altro è un aspetto fondamentale che deve essere tenuto in considerazione. Con esso tutti i parametri che ne influenzano la tenuta, come la superficie del substrato (rugosità, impurezze, morfologia), sforzi intrinseci ed estrinseci, lo spessore del film, e le proprietà meccaniche del film e del substrato risultano essere fondamentali. Infatti, è cruciale che un film riesca a mantenere il contatto con la struttura sottostante poiché possibili delaminazioni portano ad esporre il materiale ricoperto all'ambiente esterno vanificando le proprietà benefiche dei coating.

L'American Society for Testing and Materials (ASTM D907-15) definisce l'adesione come "lo stato in cui due superfici sono legate insieme da forze di interfaccia che consistono in forze di legame, di incastro, oppure la presenza di entrambe". Da questa definizione si evidenzia la complessità dell'argomento, poiché il concetto è ulteriormente estendibile ai legami chimici o fisici che si formano tra i materiali che costituiscono il film e il substrato, e il tipo di spessore dell'interfaccia che si viene a generare. Di conseguenza, l'adesione può avere diversi significati. Ad esempio, la rappresentazione termodinamica considera l'aspetto energetico dell'interfaccia per mezzo dell'energia superficiale, la rappresentazione fondamentale è il concetto ideale di somma di tutte le interazioni interatomiche tra i materiali a contatto, ed infine esiste una descrizione pratica, che tiene conto di tutti i parametri in gioco quando si forma un'interfaccia; quindi, non è solo una pura somma di forze interatomiche.

Per quanto riportato la misura dell'adesione è affetta da parecchie variabili e a causa di ciò una misura quantitativa appare una sfida. Parecchie tecniche sono state sviluppate; tuttavia, ognuna di esse ha i suoi vantaggi e limitazioni. Nel presente lavoro vengono trattate brevemente alcune di queste tecniche, evidenziando principalmente gli aspetti più critici. Viene successivamente messa in risalto con maggiore dettaglio l'analisi di materiali posti sotto ad un carico di tensione unidirezionale (prova meccanica di trazione) essendo una tecnica comunemente adottata per caratterizzare le proprietà meccaniche di un materiale. Questa tecnica viene utilizzata per studiare non solo le proprietà meccaniche di un film sottile, ma anche per valutare quantitativamente parametri caratterizzanti l'adesione attraverso lo studio e l'analisi al microscopio elettronico della formazione di cricche nel film stesso.

Un intero capitolo è stato dedicato al fine di comprendere la teoria che sta alla base della formazione delle cricche nei film sottili. L'aspetto di questa teoria è basato interamente sul concetto di energia rilasciata durante l'apertura della cricca in condizioni di stazionarietà, ovvero la cricca propaga in maniera non controllata appena viene superata una energia di frattura critica, indipendentemente dalla lunghezza iniziale della cricca. Quest'ultimo parametro è intrinseco per ogni materiale.

La cricca si innesca se nel film sono presenti difetti oppure semplicemente dai bordi del rivestimento, dopodiché può propagare verso l'interfaccia, e questo dipende principalmente dalle caratteristiche meccaniche del film e del substrato, e propagare perpendicolarmente

rispetto al carico applicato, trasversalmente lungo il rivestimento. Se la cricca riesce a raggiungere l'interfaccia, si può verificare una propagazione della cricca nell'interfaccia, che è causa principale di eventuali distacchi di film dal substrato. Un altro aspetto da considerare è che all'aumentare del carico esterno, si viene a formare un pattern di cricche con una distanza tra loro più o meno regolare. Un valore minimo di distanza e una saturazione di cricche vengono raggiunte.

Nella parte finale del lavoro, è stato descritto il caso studio dell'allumina come rivestimento contro la corrosione da liquidi refrigeranti dei reattori nucleari di IV generazione, come l'eutettico di piombo e bismuto, depositata con la tecnica a laser pulsato su substrati di acciaio austenitico. Grazie alla collaborazione con il Politecnico di Torino, è stato possibile testare questi campioni rivestiti di allumina con prove di trazione a carico crescente fino a rottura e analizzare le immagini al SEM del rivestimento nella zona di maggior sforzo. Lo studio di queste immagini non ha portato a risultati significativi in quanto questa analisi richiede un maggior numero di immagini da visionare di modo da realizzare considerazioni statistiche, oltre al fatto che è interessante valutare tale comportamento a frattura al variare dello spessore del coating. Infine, un ulteriore approfondimento di questa tematica può essere realizzato facendo uso di un'analisi computazione agli elementi finiti.

Contents

List of figures

Chapter 1 – Introduction

1.1 History of thin films

Thin film technology is simultaneously one of the oldest state-of-arts and one of the newest sciences. Thin film science is improved over the years, and nowadays it plays an important role in the development of devices ranging from energy-efficient displays to energy-harvesting and storage devices such as solar cells, fuel cells and batteries, or for corrosion protection of structural material, such as steel, from specific coolant liquids of nuclear reactors. In the future, the continuous and exponential growth of this science makes these technologies more performing.[1,2]

The idea of covering materials for specific purposes was well known. Going back in the past, the first material that it seems to be discovered before others for these scopes was gold, which was used firstly by Egyptians, primarily for decoration, ornamentations, and religious artifacts. They were able to reduce gold less than 3000 A thick (known as 'gold leaf') that could be gilded mechanically on base-metal statues and artifacts or in a particular chemical-mechanical way during the middle bronze age. This technology was called the "cold mercury" gilding process for copper and, later, for bronze objects. The interfacial layer obtained by the absorption of mercury by gold is a very early example of what is today referred to as a film/substrate adhesion layer or interfacial layer.[3,4]

Another example of a historical thin-film deposition is given by electroplating in place of metal gilding in Mesopotamia. It was found in 1936 a set of terracotta jars which contained cylinders of copper sheet and iron rods. Copper and iron form an electrochemical couple which produces a voltage, in the presence of an electrolyte. Another evidence of the past material merging with thin interfacial layers comes from the brazing developed by the Sumerians. They used as brazing materials the gold-based alloys. Finally, the last example is provided by the electroless plating, developed by the Moche Indians, who were able to join gold and silver with copper.[4]

These are a few examples of how thin films were well known and, although the technology in the past was not so well established, the idea was very clear for what concern the material protection against environment. The development of vacuum technology was essential for providing cleaner deposition environments necessary for the evolution of surface and thin film science. However, in any case, this technology suffers a lot of issues, one of these is given by the adhesion between the two materials coming from the interfacial layer. The major issue is the adhesion failure of the coating under certain conditions, and it is significant to understand the concept of adhesion for the usefulness of the film/substrate system. Before going into the details of adhesion, it is necessary to have an overview of the main deposition techniques, useful to deposit thin film by vapour phase, and the peculiar characteristics of a deposited thin film and its properties.

1.2 Review of the different deposition techniques

It is very crucial the protection of materials against severe environments and the main method is the protection with thin films in which they are deposited over the material to be protected creating a physical barrier from the external environment. This method is relatively simple due to the improvement of the research in this field.

One class of coating is provided by the electrochemistry, in which the growing film is deposited by electrodeposition. The phenomenology of this process is given by the deposition of a metallic coating by immersing the material to be protected in a liquid solution. Inside this solution, the surface of the substrate undergoes chemical or electrochemical reactions which create the coating, so this type of deposition is a wet process. In this class of deposition, we can find anodization and cromatization, however, these are out of importance for this work.[5]

Another class of thin film deposition exploits different physical phenomena using gas phases as precursors and, if necessary, using vacuum or ultra-vacuum systems. In principle, there are two main categories of deposition techniques, which differs on the type of deposition, by means, depositing thin films material from a vapor either chemically or physically. The former is based on the reaction of two gaseous species producing a non-volatile solid that deposits onto a

substrate (this technique is called Chemical Vapour Deposition CVD). In contrast, the latter is based on removing material from a target by using different physical techniques that is deposited onto a substrate (this is called Physical Vapour Deposition PVD). Thus, these two technologies are reviewed in the following sections, in particular, it will be focused the attention on a specific film deposition belonging into the physical vapor technique, the pulsed laser deposition (PLD).

The graph below shows the main techniques inside the two main categories.

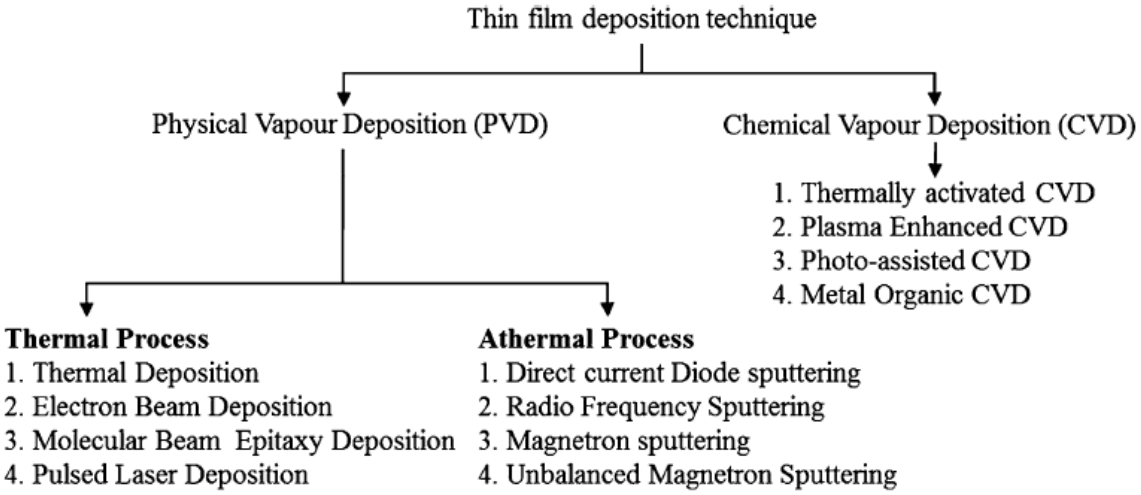

Figure 1 - List of some thin film deposition techniques[1]

1.2.1 Chemical vapor deposition (CVD)

CVD is a thin film deposition category in which the formation of the thin layer is realized after the subsequent reaction of two or more chemical species onto a surface substrate which is heated. This heated surface is the driving force for the thin film growth. This is because when the new reactive species given by the reaction of gaseous species approach the substrate to be

covered, these are adsorbed chemically or physically and can diffuse efficiently by the high temperature substrate (surface diffusion).[1,3]

Some variables must be taken into account in order to evaluate the deposition rate and the film properties, such as the substrate temperature, the precursor gas flow rate, the pressure into the chamber, the surface of the substrate, and the nature and purity of the precursor.[6]

Chemical vapor deposition is mainly a four-stage process, represented in figure 2. They are summarized the principal sequential steps as follows:[1]

- The precursor gaseous phase, or the reactant species, is introduced into the chamber together with the carried inert gas, if it is necessary
- The adsorption process in which precursor species reacts chemically on the substrate by thermal energy or plasma
- The diffusion and decomposition of the gas species on the substrate forming clusters for the following nucleation sites
- The removal of the by-product formed by the decomposition from the deposition chamber

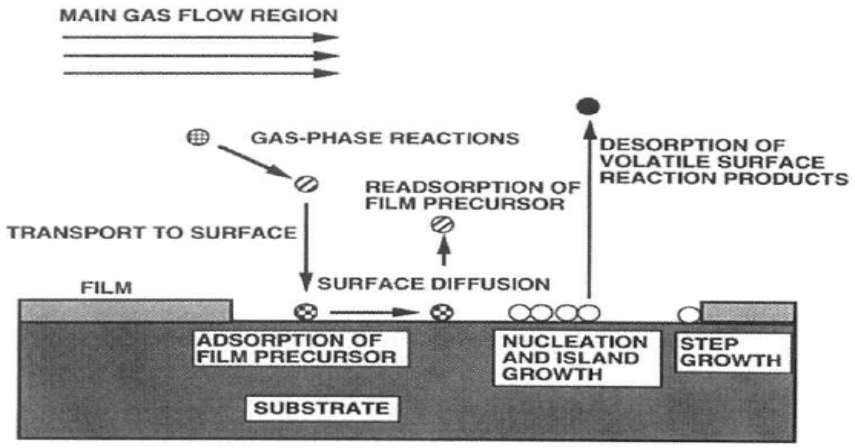

Figure 2 - Sequence of gas transport and reaction processes contributing to CVD film growth[3]

One of the reasons of growing films by CVD is the ability to produce a large variety of film made by metallic and semiconductor materials, or inorganic and organic compounds, in a crystalline or amorphous structure with a very precise stoichiometry and morphology. Based on this, there are variants of CVD technique, which differ from the activation energy of the reaction, but they will not be considered.[3,6]

The operating temperature is relatively low, and this peculiarity is so important that many substrates can be coated, and the coating is dense and pure. However, the main drawbacks of the CVD technique are chemical hazard caused by toxic, explosive, inflammable or corrosive gases, sometimes higher temperatures that are required are not compatible with the substrate, the reaction could be heterogeneous causing a lot of contamination on the deposited film and incomplete, leading an higher wastage of precursor material.[1,3]

1.2.2 Physical vapor deposition (PVD)

PVD is another deposition category in which the material to be deposited is evaporated mainly in two different ways: by thermal evaporation, where the material is heated up to a certain temperature for which the atoms have the suitable thermal energy to be ejected from the target material; or by sputtering, where the temperature of deposition is at room temperature and the energy provided for the atom ejection is given by the impact of gaseous ions. Both thermal evaporation and sputtering require high vacuum level, to avoid contaminations, thus, based on this, belonging into this category of film deposition, two subcategories can be found depending on the type of vaporization, that are thermal process, in which the deposition occurs by melting or sublimation of the target material, or athermal process, where the vaporization occurs by impact of ionized gases (sputtering).[1,3]

Also for the PVD process there are mainly four steps that are:[1]

- The target material absorbs the supplied energy
- The external energy vaporizes the target material by evaporation, sublimation, or sputtering
- The travelling of the vaporized material towards the substrate surface.
- The condensation of the vaporized material to be deposited onto the substrate

In some cases, we can have reactions of the vaporized material with the gas present in the chamber for producing oxide, nitride, and carbide thin films. Figure 3 represents the main steps for the PVD process.

It differs from CVD by the presence of molten or solid sources, instead of gaseous precursors, by the physical mechanisms either evaporation or collisional impact, by the general absence of chemical reactions in the gas phase and at the substrate surface and by a reduced pressure environment. Some advantages of the PVD are the possibility to choose the coating by using target material, form different compounds and alloys, realize thin film with a low contamination due to the vacuum in the deposition chamber, and control the morphological and crystalline parameters by setting the rate of deposition. On the other hand, technology that is behind this type of deposition requires higher costs, the thickness of the film is not homogeneous over the surface, moving from the centre to the edges, and poor step coverage and shadowing are present during the deposition.[1,3]

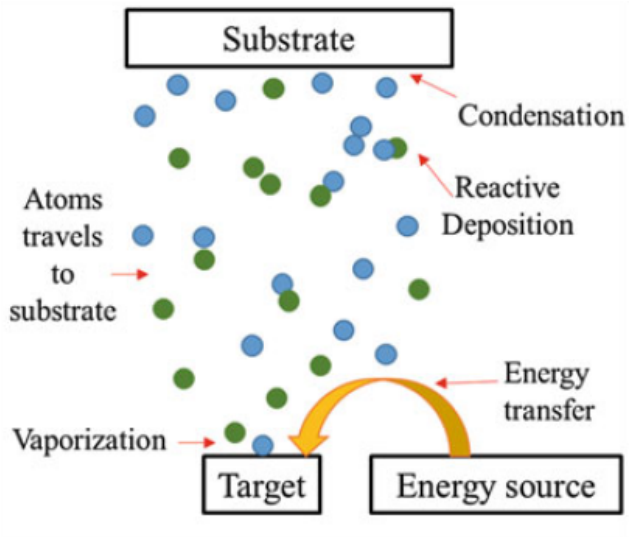

Figure 3 - Representation of the main steps in a PVD process[1]

Among the different PVD approaches, a versatile deposition technique that is worth mentioning is the so-called Pulsed Laser Deposition (PLD), which is the principal one of the present work. PLD belongs to the subcategory of the thermal deposition process because a pulsed laser beam vaporizes the target material.[1] It is based on highly energetic pulsed laser in the range typically of the ultraviolet that hits repeatedly a target of the source material that we want to grow as thin film with a controlled frequency. During this irradiation, it forms a plasma plume perpendicular to the target, which consists of a distribution of species, like atoms, molecules, electrons, ions, clusters, particulates, and molten droplets.[7,8]

The process of deposition can be summarized in three main steps: ablation, plume propagation, and deposition. In the ablation step, there is laser-matter interaction in which the expulsion of atoms, particles and even droplets can happen if the laser beam power is higher than the ablation threshold. In this stage we have a distribution of particle sizes which move with different velocities forming the ablation plume, and for the thin film deposition it is extremely important to avoid big clusters and droplets reach the substrate surface. Then, we have the propagation and, depending on the gas pressure inside the chamber, the plume can have different sizes because the particles inside the plume interact with each other and with the particles of the gas leading to lateral and longitudinal expansions. Moreover, particles can decrease their velocity or deflect their trajectory due to collision. In this step, we have not only elastic collisions but also inelastic collisions, which bring particles to aggregate with each other and increase their size, so it is important to control the pressure and the type of the gas inside the chamber. Finally, we have the deposition stage in which the particles in the plasma interact with the substrate surface. This last step, in addition to the substrate temperature, is fundamental for the growth and the microstructure of the film, and thus on its mechanical properties.[9]

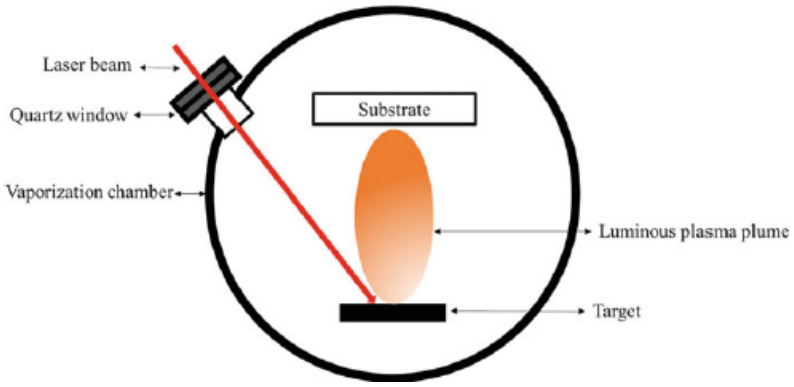

Figure 4 - Representation of the pulsed laser deposition[1]

A typical PLD configuration is realized by a chamber where it is located the target of the source material and the substrate, over which the growing film will develop. Laser beam is located outside the chamber, and it is focalized by specific lenses on the target with a tilted angle less than 45° respect to the perpendicular of the substrate surface. The chamber could be in ultrahigh vacuum or with a controlled background gas pressure.[9] A schematic representation of the PLD configuration is shown in the figure 5.

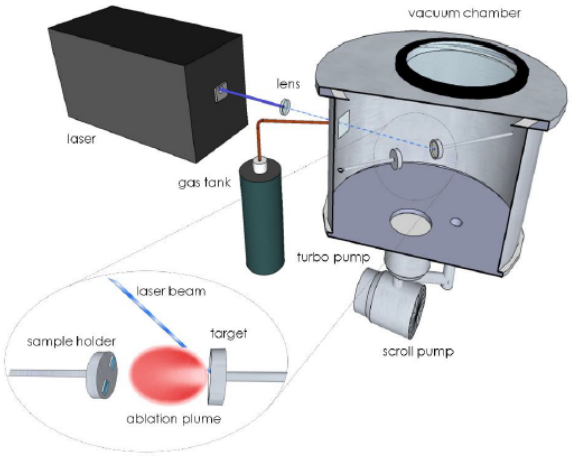

Figure 5 – Configuration and setup of the PLD[10]

An advantage of PLD is the possibility of producing nanoparticles, which can nucleate and grow into the ablation plasma during the propagation stage. The growing of nanoparticles is divided in two processes, the formation and the growing of nuclei. The number of nuclei depends on temperature and pressure, but the condensed nuclei depend on the material available for the growing, so the formation and the growth of nanoparticles are competing processes. The most important parameter for controlling the particle size distribution is the cooling rate, which in turns depends on the pressure gas and the temperature in the chamber. A decreasing temperature leads to an increasing of the nuclei formation with higher rate than the particle growth, so a faster cooling speed results in a higher number of particles, at the same time, a decreasing pressure leads to a decreasing in growing rate, thus, the size distribution.[7,8]

Although PLD is considered as a thermal process by the fact that the absorbed laser beam vaporizes the target material[1], this technique is largely considered as a nonthermal deposition, that is, when the laser is absorbed by the target, energy is first converted to electronic excitation in a local non-equilibrium interaction between radiation and target material, and then into thermal, chemical, and mechanical energy, resulting in evaporation, ablation and plasma formation.[8,11]

1.3 A general overview of thin films

In the previous section a wide overview of the main deposition categories is made, focused the attention on a specific deposition technique, which is the aim of this work. Before describing the growth of a coating, it is essential to define a thin film.

A thin film (also called as layer or coating) can be defined as a near-surface region whose properties are different from those of the bulk of a material, and it can be stated a maximum of thickness of about a few microns or less. Thus, controlling the thickness of the growing film is very important in order to consider the properties of a particular material grown as thin film. The properties also depend on the substrate nature, and deposition conditions.[6] Moreover, the structure of the growing film is another significant parameter, in particular the grain size, the morphology, and the crystallinity, and all these are influenced by the deposition techniques, the

temperature, the crystallinity of the substrate and so on. So, first of all, it is essential to highlight how thin films grow.

1.3.1 Modes of film nucleation and growth

Once the deposition of the coated material onto the substrate is initiated, the atoms rearrange and it has been recognized that three basic types of growth exist:[3,11,12]

- The layer growth (also called Frank-Van der Merwe growth), in which is favour the growth of planar monolayer, in particular the first monolayer has to be completed before the next one since the particles of the coated material are strongly bonded to the substrate to each other (fig. a)
- The island growth (also called Volmer-Weber growth), in which the growth of small clusters is the primary growth mechanism, and it occurs when the growing film's particles are strongly bonded to the substrate (fig. 6b)
- The Stranski-Krastanov growth, which is the combination of layer-by-layer growth followed by island formation (fig. 6c).

The mode in which the film grows follows pure thermodynamic conditions, in particular thin film morphology needs a balance between the free surface energies of the film, the substrate, and the interface between film and substrate. In general, looking the figure 1, if the sum of the interface and film surface energies is lower than the substrate surface energy, i.e., $\gamma_F + \gamma_I < \gamma_S$, a layer-by-layer growth is the principal growth's mechanism, because strong bonding between film and substrate reduces the interface surface energy. On the contrary, no bonding between film and substrate promotes island growth.[11,12]

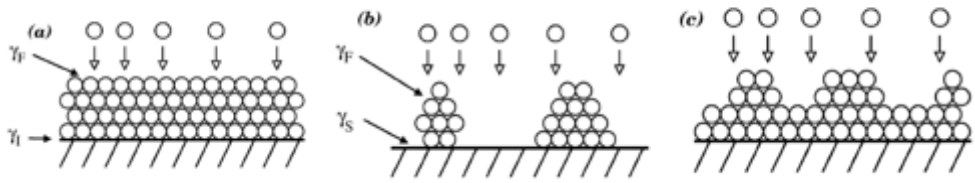

Figure 6 - Different types of film growth[12]

1.3.2 Film structures

The growing film follows the substrate structure and its temperature. Based on these conditions, the film grows forming its microstructure (crystalline, polycrystalline, or amorphous), which is highly dependent on the deposition parameters and techniques. Sometimes, it is possible to obtain a microcrystalline structure, consisting of nanoparticles larger few tens of angstrom embedded in an amorphous matrix.[11] Controlling the microstructure of the growing film has important consequences for what concern the properties of the coating itself. For example, a columnar morphology, which develops in amorphous films, often has internal defects and voids, or porosity distributions, that are detrimental to the mechanical properties.[3]

There are models, the so-called structure zone models (SZMs), which are used to understand well the microstructure of the growing thin film depending on the deposition and substrate parameters. It was proposed a SZM by Movchan and Demchishin based on the normalized substrate temperature $T = T_S/T_M$ where T_S is the substrate temperature and T_M is the melting temperature of the coated material. An increase of T corresponds to a better surface diffusion.[3,11]

From this model, it can be defined three zones:

- $T_S/T_M < 0{,}3$, where the film presents a columnar structure with high porosity
- $0{,}3 < T_S/T_M < 0{,}45$, where the film presents again a columnar structure, but they are narrow with less porosity
- $T_S/T_M > 0{,}45$, where the film presents an equiaxed grain structure due to an excellent diffusion mechanism.

Thornton proposed another zone scheme for sputtering deposition, which is similar to the previous one. However, here there are four zones: zone 1, T, 2 and 3, where zone T is considered as a transition region between zone 1 and 2. This model takes into account the gas pressure. For ceramic materials, it is discovered that they are softer for low value of T_S/T_M, while they become hard in zone 2 and 3.[3]

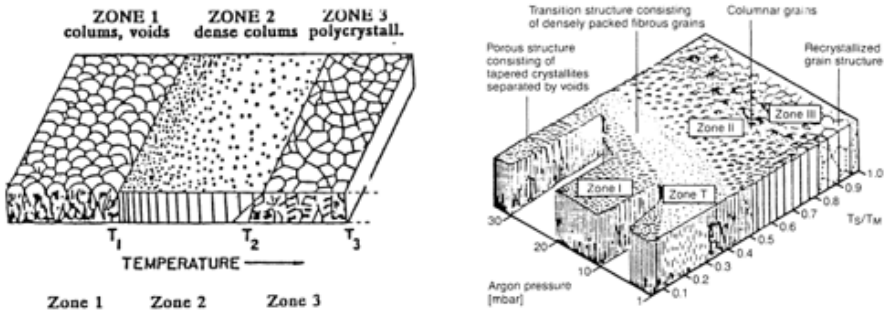

Figure 7 - Structure zone model of Movchan and Demchishin (left) and of Thornton (right)[13]

It is of paramount importance to consider more variables for better control of the thin film growth and microstructure, and a study that considers more variables is provided by K. Guenther. From this study, Guenther proposed an extension of the original SZM, so that it can be possible to take into account the dense, amorphous microstructure as a fourth zone beyond the normalized substrate temperature $T_S/T_M = 1$. The physical interpretation of this zone is to consider the mean thermal energy of the incoming particle's total energy being higher than the melting temperature of the bulk material.[13,14]

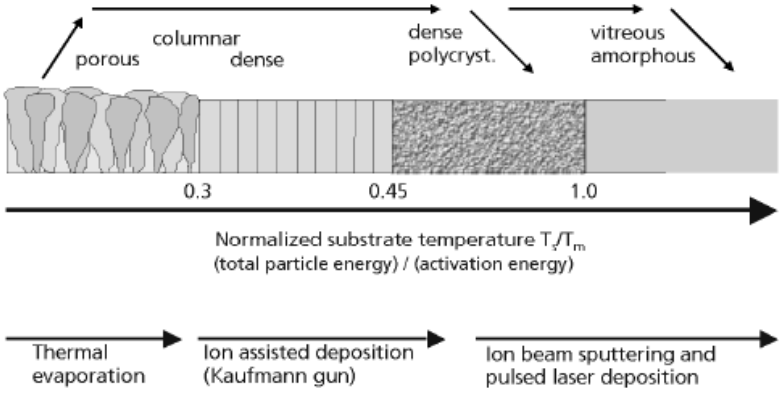

Figure 8 - Extended and generalized structure zone model of thin film growth[13]

1.3.3 Internal stresses

The films, when grown onto a substrate, develop internal (or residual) stresses. These stresses can be detrimental to the application for which the film/substrate system is used because they are sometimes sources of cracking, or, in the worst situation, they can peel off the film from the substrate, compromising the properties of the film during service life due to stress relaxations. This scenario is present if these stresses are equal to or above the yield stress of the bulk material. It is crucial to consider and measure the formation, the level, and the sign (stresses could be either tensile or compressive) of stresses during and after the deposition.[15,16]

The residual stresses include two types of stresses:

- The intrinsic stresses are developed following the growth during the deposition process and are due to the presence of defects, surfaces, and interfaces. The interface between the film and substrate accommodates the lattice mismatch between the lattice parameter of the film and the substrate. Another source of intrinsic stresses is the presence of impurities or adsorbed molecules onto the substrate. These stresses are unavoidable
- The extrinsic stresses, which are developed principally due to the difference on thermal expansion coefficients of film and substrate and occurs when there is a change from the deposition temperature to the room temperature.

Stresses can be either tensile or compressive, and in general the stress sign depends on the type of deposition technique performed to grow the coating. For example, for thermal evaporation, the substrate temperature plays an important role in establishing the sign due to the surface diffusion of the depositing atoms. For low temperatures, stresses are typically tensile, while for higher temperatures, stresses become to be compressive.[3,15] An example is given by Thurner et al with the thermal deposition of chromium film onto MgF_2 substrate varying the substrate temperature, that is represented figure 9.[17]

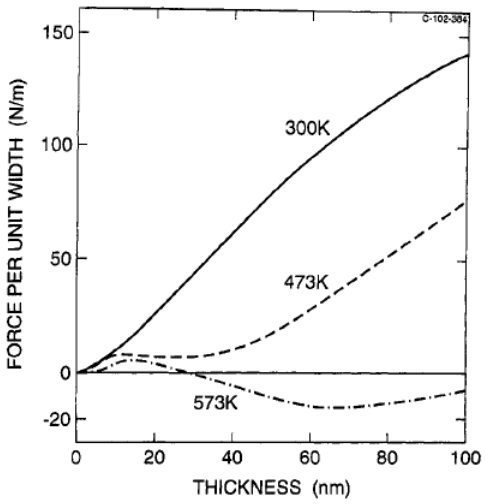

Figure 9 - Deposition of chromium thin film with different substrate temperature[17]

For sputtering deposition, the stress is mainly compressive due to the atomic peening, that is, the continuous bombardment of the growing film with high-energetic particles recoil-implants the surface atoms of the layer and these new implanted atoms occupy small spaces than the usual atomic volume. The compressive stresses arise with increasing particle energy.

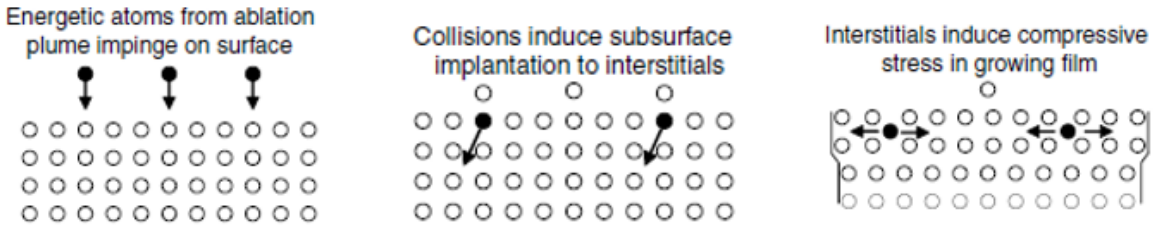

Figure 10 - Schematic representation of the compressive stress by PLD[7]

Another important consequence of the internal stresses is the bending of the film/substrate system. If the film is in a tensile state of stress, the substrate balances this stress with compressive forces, but, since remains moment unbalancing, the system tends to bend concavely upward, vice versa, a compressive stress film bends the system convexly downward. Significant tensile stresses cause film cracking and fracture, while large compressive stresses cause film wrinkling and local loss of adhesion.[3,15]

Finally, residual stresses are strongly dependent on the film thickness, and it is demonstrated that there is a critical thickness for which it is thermodynamically favourable for the film to elastically relax, losing the perfect lattice matching at the interface between film and substrate.[16]

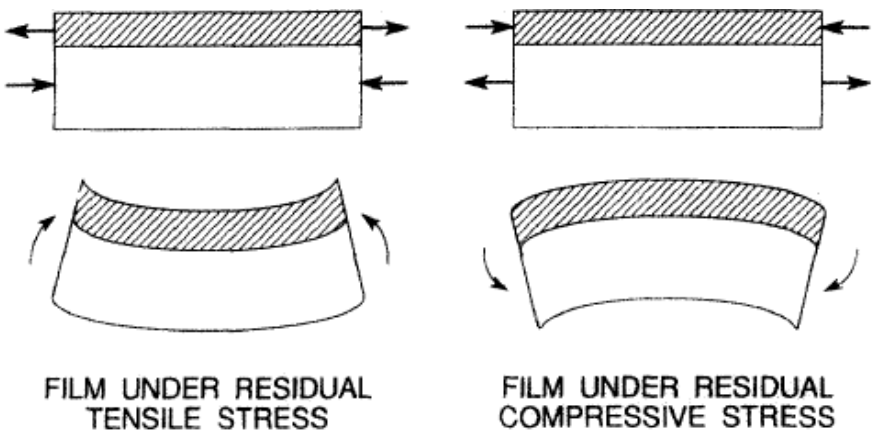

Figure 11 - Bending film-substrate system under a) tensile stress and b) compressive stress[3]

In conclusion, the sources of the internal stresses are diversified. The principal ones of these are the difference in thermal expansion coefficients of film and substrates due to change in temperature, incorporation of different atoms respect to the growing film (e.g., impurities), lattice mismatch between film and substrate lattice parameters, recrystallization processes and arrangement of dislocations.

Here, it is reported some general values of internal stresses:[3]

- Evaporated metal films are in tensile stresses of about 1 GPa
- Sputtered metal films have stresses of about 2/3 times higher than evaporated ones
- Nonmetallic films (insulators and semiconductors) are in a state of compression of hundreds of MPa (100-300 MPa).

1.4 Adhesion of thin films

To estimate the mechanical properties of a thin coating, the best solution is to realize free-standing thin films. For its purposes, Haque et al. used lithography and micromachining techniques to pattern the specimen and to release it from the substrate. In general, it is quite challenging to realize this type of sample, in fact, the problems are the fabrication of free-standing and stress-free specimens, the manipulation of the specimen during the test, and the generation of minimal forces that can be detected, thus the only way is to attach the material as a thin film to the substrate.[18]

Although this can be a problem for the characterization of thin film mechanical properties since the coating is affected by the substrate, particularly by the interaction between the film and substrate, the scope of the present work is to evaluate the capability of the coating material to remain attached to the substrate. This physical mechanism is called adhesion and ASTM D907-15 defines it as “the state in which two surfaces are held together by interfacial forces which may consist of valence forces or interlocking forces, or both”.[19]

From a microscopic point of view, once the atoms of the film approach the substrate atoms, we can have bonds of different natures between different kinds of atoms, obtaining pairwise interactions across the interface. Based on the binding energy, there are two types of adhesion forces: physisorption (which involves Van der Waals forces) and chemisorption (which involves metallic, ionic, and covalent forces). They are adsorption processes and differ based on the atomic interaction strength. The energy involved in the physisorption process is about 0.1-0,5 eV per bond, while in the chemisorption process is about 1-10 eV per bond.[3,20]

From a thermodynamic point of view, this concept is clearly explained by the surface energy theory. If we define γ_F and γ_S the specific surface energy of film and substrate, respectively, and γ_{FS} the interfacial energy, then the work required to separate the two surfaces per unit area W_A (called as work of adhesion) is given by:

$$W_A = \gamma_{F+}\gamma_S - \gamma_{FS}$$

W_A represents the energy difference between the two separated surfaces and the two surfaces in contact; thus, if W_A is positive, adhesion is present, and it represents the work necessary to create two new surfaces.[3]

Finally, from a macroscopic point of view, one needs to measure adhesion as a physical property quantitatively. However, several factors that influence adhesion have to be taken in consideration, for example, the substrate preparation (roughness, porosity, cleaning etc.), the deposition condition, the properties of substrate and film materials and aging.[20]

1.4.1 The interfacial layer

When the interaction of the two heterogeneous materials is established, a new zone could be created, which is called interfacial layer. The adhesion properties strongly depend on the microstructure of this zone.

Five types of interfacial layers exist:[20-22]

- The mechanical interface layer, which depends on the porosity and roughness of the substrate (fig. 12a)
- Monolayer on monolayer, which is a very thin layer, with 2-5 Å thickness, and no chemical reaction and diffusion are involved (fig. 12b)
- The chemical bonding interface layer is characterized by constant chemical composition, and chemical reactions are involved (fig. 12c)
- The diffusion interface layer is characterized by a constant change in the lattice and composition in this transition layer. Forming this layer needs external energy (e.g., from evaporation) to favour diffusion (fig. 12d)

- The pseudodiffusion interface layer, which is characteristic for depositions with higher energy particles, and in this layer, there are several point defect concentrations and stress gradients (fig. 12e).

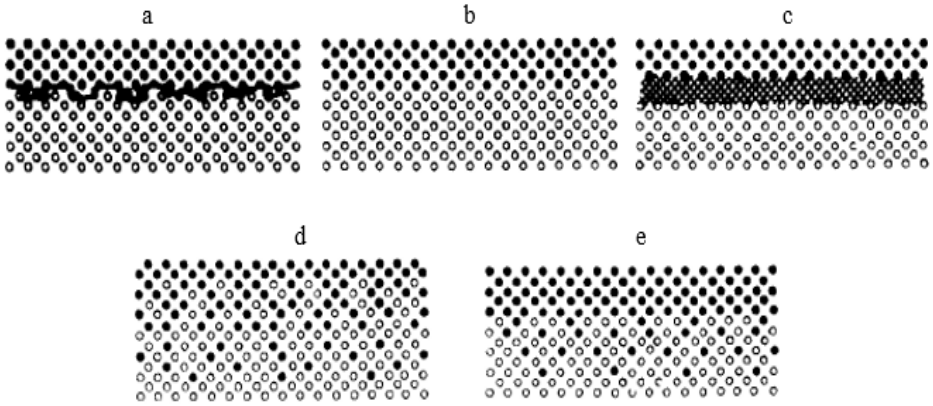

Figure 12 - Different types of interfacial layers[21]

In general, an interface is considered a new region with its own mechanical properties that must be evaluated if we want to estimate if the adhesion of the two materials is efficient or not. Based on the interfacial type, we can define if this can be a very sharply or a very diffuse interface layer. This concept is schematically depicted in figure 13.

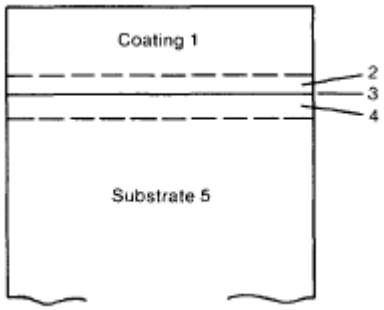

Figure 13 - Five regions of the generalized film/substrate system[21]

Another critical aspect of the film/substrate interface is strongly influenced by the coating and substrate lattice parameters. If there is a perfect lattice matching, i.e., the lattice parameters are similar, then the interface is free of defects, and it is referred to as coherent. In contrast, a lattice mismatch produces a coherently strained film provided the substrate is thicker than the coating. In this case, a parameter is introduced to describe this situation, the misfit strain parameter m

$$m = \frac{a_s - a_f}{a_f}$$

Where a_s and a_f are the bulk substrate and film lattice spacings, respectively. A formation of an array of dislocations at the film/substrate interface can accommodate the misfit. Once the film becomes thicker, its lattice constant starts to approach the bulk value so the lattice mismatch becomes significant, generating edge dislocation defects at the interface. [11,16]

1.4.2 Adhesion measurements

Adhesion can be manifested in three different ways and based on these one could take adhesion measurements: thermodynamic, fundamental, and practical adhesion. Thermodynamic (or reversible) adhesion is related to the change in free energy when an interface is formed (or separated).

Thermodynamic adhesion is expressed in terms of work of adhesion W_A as:

$$W_A = \gamma_{F+}\gamma_S - \gamma_{FS}$$

The fundamental (or basic) adhesion FA can be defined as the summation of all interfacial intermolecular interactions between the contacting materials. It can also represent the energy required to break chemical bonds at the weakest plane in the film/substrate system. These two definitions are different since the former represents contact formation, while the latter represents contact break, and the weakest disruption plane may not be where the contact is initially formed. The practical (or experimental) adhesion PA is the force, or the work required to remove or detach a film from the substrate irrespective of where the localized failure occurs;

that is, it is the measurable adhesion with techniques in which the maximum force per unit area required to separate a coating from its substrate is determined. [23,24]

Practical adhesion differs from fundamental adhesion for several other factors, such as stresses into the film, thickness and mechanical properties of the coating, mechanical properties of the substrate, mode of failure, work consumed by plastic deformation, and the technique used for adhesion measurement and its parameters. Thus, one could expect that fundamental adhesion values are always the same, while practical adhesion values always differ. However, fundamental adhesion is not very useful since it is impossible to calculate the magnitude or measure such adhesion forces in practical systems. In general, one can describe this as:

$$PA = FA - IS \pm MSM$$

Where IS is the internal mechanical stress and MSM is the method-specific measurement error. Consequently, practical adhesion is not a universal value that could be measured because of the unknowing size of the measurement error and other factors.[20,23]

The issue highlighted in previous discussions is that coating is bonded with its substrate by forces of different nature so making measurements of the thin film adhesion is not trivial. Of course, when one takes adhesion measurements, it must take into account the destructive measurement techniques corresponding to film detaching from the substrate and then the subsequent measurement of the strength that holds film and substrate together. There are several techniques for studying adhesion, and one of these depends on different factors such as the thin film thickness, residual stresses and the mechanical properties of film and substrate. Experimentally, adhesion can be measured in two ways:[19]

- The adhesion strength measurements, which define the maximum force per unit area exerted when the two materials are separated
- The interfacial toughness measurements, which define the work of adhesion as the work done in separating two materials from one another, or, in other words, the energy dissipated per unit area upon extending a crack along the interface.

Chapter 2 – Theory of thin film cracking

As it has been described so far, performing adhesion measurements is quite complex since many factors influence adhesion because it depends on the type of interface established between film and substrate. The interface is an intrinsic property of layered materials as film-coated substrates, and the importance of considering the mechanical properties of interfaces will be the keystone for the following. The theory of crack nucleation and propagation in thin films/thick substrate composites will be treated. These layered materials are susceptible to interface debonding or delamination, and, in general, cracking of a layer is possible when tensile stresses are developed. At the same time, buckling can occur when stresses are compressive.[25]

We have seen that the deposition of thin films onto substrates causes the appearance of unavoidable intrinsic stresses (tensile or compressive), which may provoke the presence of different crack morphologies. When we consider a film/substrate system under tensile stress, given by intrinsic or extrinsic stresses, higher enough to promote nucleation and propagation of cracks, there are mainly five types of crack patterns that we can find:[25,26]

- Surface cracks, which nucleate from flaws, and arrested by the interface, so the external stress is not high enough for the crack to channel through the film (fig. 14a)
- Channeling cracks, which are highly unstable, because, once activated, they would never arrest until it encounters another channel crack or an edge (fig. 14b)
- Substrate damage cracks, which are cracks in the film propagated further into the substrate. Such cracks may be stabilized at a certain depth (fig. 14c)
- Substrate spalling cracks, which are cracks that select a path at a certain depth parallel to the interface (fig. 14d)
- Debonding cracks, which initiate from edge defects or channel bottoms (fig. 14e)

If the stresses are compressive, the presence of buckling could be found in thin films. There are two possible types of buckling: wrinkling (fig. 15a), in which no delamination occurs but the substrate deforms coherently with the film, and buckle-delamination (fig. 15b), in which the film is partly delaminated from the substrate. For the thin elastic film, wrinkling is possible if

the substrate is relatively compliant since it requires coherent deformation, while for stiff substrate, the buckling deformation of the film highly constrained could happen, although the substrate constraint may be locally mitigated by interfacial defects that lead to partial delamination of the film. The onset of buckling and the buckling mode depend on the elastic mismatch between film and substrate and the pre-existing interfacial defects.[27]

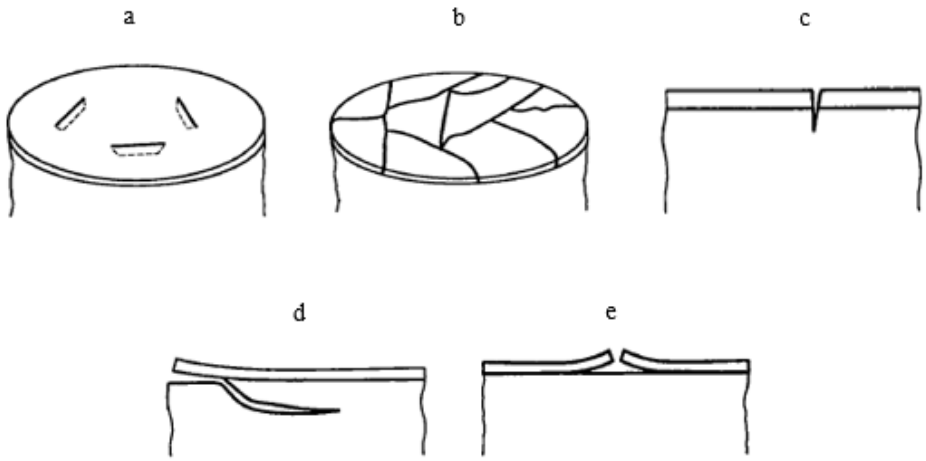

Figure 14 - Commonly observed cracking patterns under tensile stress[26]

Our goal is to describe the formation of a crack in the film under applied tensile stress, assuming that no cracks are formed in the substrate. Then, if a crack is formed into the coating, the crack propagates towards the interface, channeling for perfectly elastic and isotropic materials, and the specific case of ductile substrate will be discussed. Finally, the formation of an array of parallel cracks perpendicular to the applied loading is considered.

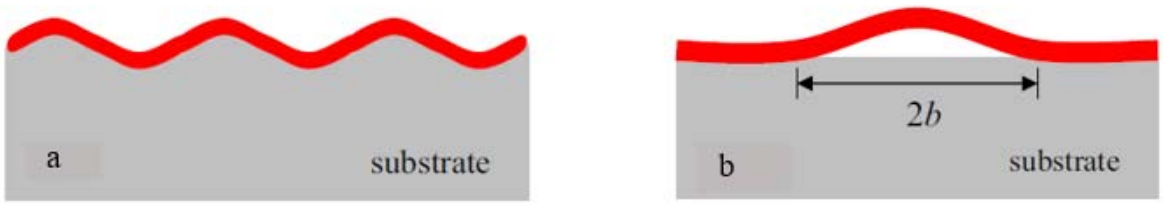

Figure 15 - Thin film failure under compressive stress[27]

2.1 Mechanical properties of bulk materials

Before going into the details about the film cracking under external forces and the techniques to measure adhesion quantities, it is useful to overview the most important mechanical properties. This section is very useful to understand the mechanical properties of the film and substrate separately, and the importance to combine them as a unique body due to the strong interaction generated by the formation of an interface.

2.1.1 Stress-strain curve by uniaxial tensile testing

One of the most important techniques for measuring material properties is the uniaxial tensile testing, from which mechanical parameters could be recovered by analysing the experimental stress-strain curve, which is represented in figure 16.

This test consists of applying a unidirectional loading (for the convention in the z direction) perpendicular to the sample cross-section. The load F and the elongation u are normalized by the engineering stress σ and the engineering strain ε, respectively. The stress is defined as the ratio of the load F and the initial sample cross section A_0 ($\sigma = F/A_0$), while the strain is defined as the ratio of the change in length Δu and the initial length u_0 of the specimen ($\varepsilon = \Delta u/u_0$) along the z-direction.[28]

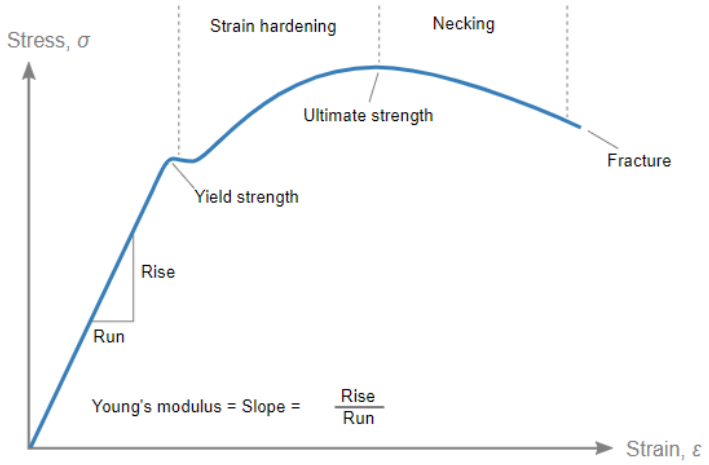

Figure 16 - Typical stress-strain curve of a specific material[29]

At the initial stage, the sample is stretched elastically by the uniaxial tensile loading. Here, we are in a region where, after removing the load, the specimen recovers its geometry without any permanent deformation. In this situation, the sample elongates along the direction of the applied force, while it contracts in the lateral directions, perpendicular to the load. Microscopically, the elastic deformation involves interatomic bond stretching.[3]

In this stage, three important mechanical properties could be derived, under the assumption of isotropic materials:[28]

- The elastic modulus E (called Young's modulus) is the slope of the first part of the stress-strain curve (the elastic region). The constitutive equation that links stress σ and strain ε is linear and obeys Hooke's law:

  $\sigma_z = E\varepsilon_z$

  This material property represents the stiffness of the specimen. The material with a higher elastic modulus is stiffer or less compliant than the material with a lower elastic modulus.

- The Poisson's ratio ν, which is the ratio of the lateral contraction ε_x or ε_y and the axial strain ε_z:

  $$\nu = -\frac{\varepsilon_x}{\varepsilon_z} = -\frac{\varepsilon_y}{\varepsilon_z}$$

  The negative sign is imposed because the strains in the lateral directions are negative, so the Poisson's ratio is always a positive quantity. Moreover, Poisson's ratio ranges from 0, which, in principle, characterizes the highly deformable materials, to 0,5 which, in principle, characterizes the incompressible materials. We neglect materials with negative Poisson's ratio
- A third quantity is derived knowing the elastic modulus and the Poisson ratio, that is the shear modulus G, which is related to the shear stress τ, originated by shear forces parallel to the material cross-section:

  $$G = \frac{E}{2(1+\nu)}$$

Then, if the external stress overcomes the yield strength σ_y, which is a specific material property, specimen falls into the plastic region, where any subsequent deformation cannot be recovered, leading the sample to be deformed permanently. Plasticity is difficult to model mathematically because the material response is nonlinear, but there are several models which easily describe this behaviour.[3]

Finally, when the stress reaches the maximum possible value for a specific material, the specimen starts necking, in which the cross-section of the specimen decreases more and more up to the final fracture of the specimen. During this transition, two important parameters can be derived: the ultimate tensile strength σ_{UTS}, which is the maximum stress in the stress-strain curve, and the percentage of elongation up to failure, which is the ratio between the variation of the specimen length after the fracture and the initial lenght.[28]

2.1.2 Brittle and ductile behaviour

We have considered the general behaviour of a material under uniaxial tensile stress. However, the difference in the behaviour can be analysed after the fracture by comparing the stress-strain curves of the materials. A material is defined ductile if it can deform with high elongations as soon as the applied stress overcomes the yield strength of that material, and the specimens exhibit substantial plastic deformations before rupture. On the contrary, a material is defined brittle if little or no plastic deformation is shown. In this case the value yield strength value cannot be precisely derived. These two trends are depicted in figure 17.

From an energetic point of view, a ductile material absorbs more energy from the applied stress with respect to the brittle one. This is shown by the area below the stress-strain curve that represents the energy absorbed by the material per unit volume. This concept is fundamental concerning the crack nucleation and propagation inside the specimen that brings it to the final fracture. In fact, in a ductile material, the crack propagates slowly since the plastic flow processes inside the material consumes the energy due to the stress redistribution at the crack tip. At this point crack propagation is stable up to a spcific value of the applied stress (the ultimate tensile strength) over which the crack becomes unstable. On the other hand, in a brittle material, the nucleated crack is always unstable, and the propagation occurs instantaneously, leading to a catastrophic fracture.[28]

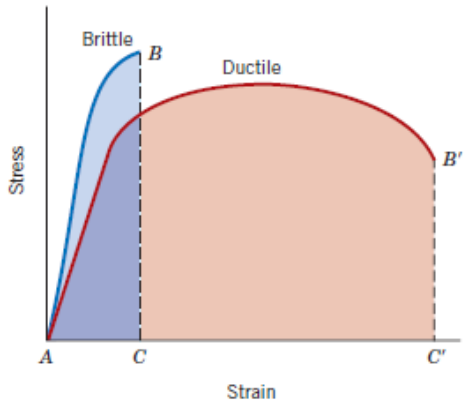

Figure 17 - Representation of tensile stress/strain behaviour for brittle (blue) and ductile (red) materials after fracture[28]

2.1.3 Stress intensity factor and fracture toughness

The importance of considering the nucleation and the propagation of cracks inside material is strictly related to the usefulness of that in service. For example, for structural steel coated by a ceramic thin film, cracks in the film expose the underlying steel to be in contact with corrosive agents from the external environment causing it to deteriorate.

The mechanical analysis of cracks falls into the mechanical fracture theory, which is based on the concept of stress concentration at the crack tip. Once a sample is loaded in tensile stress, cracks that are generated into the bulk material act as stress magnitude amplifiers near the tip; that is, the externally applied stress increases locally in value. If cracks have an elliptical shape, as it is shown in figure 18, the maximum stress σ_m at the crack tip reads:

$$\sigma_m = 2\sigma_0 \sqrt{\frac{a}{\rho_t}}$$

Where a represents the crack length, σ_0 the externally applied stress, and ρ_t the curvature radius of the crack tip. Of course, not only microscopic defects are the source of cracks, but also sharp corners, inclusions, scratches, and notches.[28]

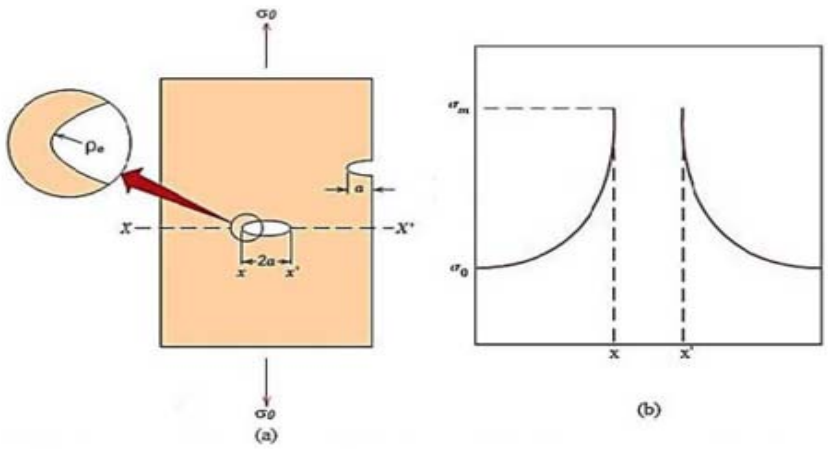

Figure 18 - a) Geometry of the crack and b) stress distribution in the section X-X' [28]

It can be noticed from the previous equation that sharper tips of the defects, i.e., low curvature radius values, are more critical in terms of stress amplifiers, thus, the presence of defects and their geometry inside the material are the leading causes of material failure. In brittle materials this effect is more evident than in ductile ones, since the stresses in ductile materials are redistributed around the tip by plastic flow. Based on this observation, it is useful to introduce the concept of stress intensity factor K, which describes the stress distribution around a flaw and the stress increase near the tip. A general formulation of this quantity is given by:

$$K = \alpha\sigma_0\sqrt{\pi a}$$

Where α is a parameter that depends on the specimen and cracks geometry, and an analytical expression of this parameter could be derived for each crack configuration. Sometimes, mathematical expressions of α are pretty complex, but, if cracks are much shorter than the specimen width, e.g., a plate of infinite width having a through-thickness crack, $\alpha = 1$.[28,30]

Another point to consider is the mode in which the applied external forces open cracks: mode I or tensile mode refers to a tensile stress applied in the direction perpendicular to the faces of the crack (fig. 19a), mode II or sliding mode refers to a shear stress applied normal to the leading edge of the crack but in the plane of the crack itself (fig. 19b), and mode III or tearing mode refers to shear stress applied parallel to the leading edge of the crack (fig. 19c).[30]

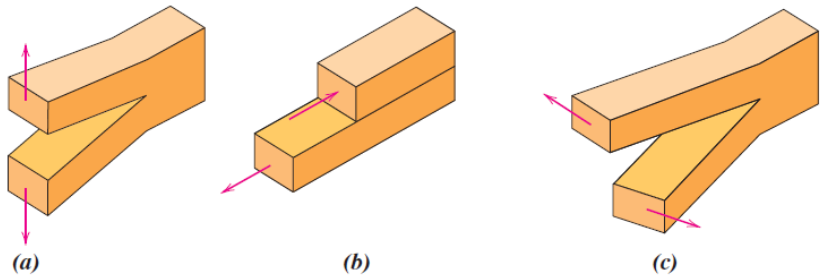

Figure 19 - The three modes of crack surface displacement[28]

So, for each of these three modes, a different stress intensity factor could be associated, and the most used is the stress intensity factor in mode I, labelled as K_I. Moreover, the stress intensity factor depends on the thickness of the specimen, and the lowest value is given by thicker specimens, which is the most severe stress state condition, so this is considered as the critical stress intensity factor (K_{IC}), which is called fracture toughness. This parameter is very important in fracture mechanics, because it is independent on crack length, geometry and loading condition, it depends only on the material.[30] Definitely, fracture toughness is the critical stress intensity factor in mode I loading measured in plane strain condition and it refers to stress resistance of a material to fracture in presence of flaws or higher stress intensity that a material can withstand without fracture.[19]

2.1.4 Energy release rate for crack propagation

Fracture mechanics can be explained from an energetic point of view, which is introduced for the first time by Griffith, who considered that the deformation energy given by the applied stress can be transformed in fracture energy. Basically, the critical fracture condition is set as the equilibrium condition in which the crack forms, or grows if it is already present, without total energy variation. A crack is driven by the relaxation of stresses and the consequent decrease in energy stored in the system. We define the energy release rate G as the energy needed to create two new surfaces (it is the driving force for crack propagation), and, in general, is given by $G = -dU/dA$, where U is the stored elastic energy and A is the crack area. The energy release rate is related to the stress intensity factor K as derived by Irwin:[31,32]

$$G = \frac{K^2}{\bar{E}}$$

Where $\bar{E} = E$ in plane stress condition, or $\bar{E} = E/(1-\nu^2)$ in plane strain condition, while K could be or not the combination of the three fracture modes K_I, K_{II}, and K_{III} as:

$$K^2 = K_I^2 + K_{II}^2 + K_{III}^2$$

Thus, G can be calculated from elasticity for any hypothesized mode of failure. However, the fracture will occur if the driving force exceeds the fracture resistance, which consists not only of the energy required to create new surfaces, but also of any irreversible loss, such as plasticity.[32]

As it is introduced previously, for homogeneous solids, fracture toughness is defined as the critical value of K_I determined by a valid test of a mode I specimen, denoted by K_{IC}. In particular, for elastic results to apply any plasticity must be confined to a small region at the crack tip, and this condition is referred to as small-scale yielding. Equivalently, one can use the critical value of G as the toughness, where the critical G will be denoted by Γ_C, which is fracture resistance. For mode I, the two toughness measures are related by:[25]

$$\Gamma_C = \frac{K_{IC}^2}{\bar{E}}$$

2.2 Mechanical properties of a film/substrate system

So far, it has been made a brief analysis of the principle mechanical properties of solid homogeneous and isotropic materials. However, we are interested in evaluating what happens when two materials are joined together, as in the case of film coated substrate. The description of cracks in a combination of two or more materials joined together is different from the cracks that appears in a single bulk material, but in both cases, they appear when inside the material there are some defects or discontinuities or when they are provoked by the presence of boundaries or edges. The difference is that the composite has to be considered as a unique body with three different regions: the film, the substrate, and the interface, all with their mechanical characteristics.

2.2.1 Dundurs parameters

Let's consider a thin film bonded to a thick substrate which are isotropic and linear elastic. These two hypotheses are very important since now we consider only a pair of elastic properties for each material involved in the composite system (e.g., Young modulus and Poisson ratio), and no plastic deformation is present. Again, we analyse this system under uniaxial stress tension in a plane condition.

For such a problem the stress field generally depends on three parameters formed from the elastic constants, for instance, the ratio of the shear moduli ($\Gamma = G_f/G_s$) and the Poisson's ratios of the film (ν_f) and the substrate (ν_s), but, Dundurs (1969) observed that this problem could be reduced using only two parameters, the so-called Dundurs parameters, α and β, expressed as:[33,34]

$$\alpha = \frac{\Gamma(k_s + 1) - (k_f + 1)}{\Gamma(k_s + 1) + (k_f + 1)}$$

$$\beta = \frac{\Gamma(k_s - 1) - (k_f - 1)}{\Gamma(k_s + 1) + (k_f + 1)}$$

where k_i represents a constant depending on the Poisson ratio, and it is different if the problem is either plane strain or plane stress conditions (the subscript i stands for film or substrate):

$$k_i = 3 - 4\nu_i \quad (for\ plane\ strain)$$

$$k_i = \frac{3 - \nu_i}{1 + \nu_i} \quad (for\ plane\ stress)$$

A better formulation of the Dundurs parameters is given by Beuth. This is used in many works since this formulation shows the elastic mechanical properties of both materials explicitly:[35]

$$\alpha = \frac{\bar{E}_f - \bar{E}_s}{\bar{E}_f + \bar{E}_s}$$

$$\beta = \frac{G_f(1-2\nu_s) - G_s(1-2\nu_f)}{2G_f(1-\nu_s) + 2G_s(1-\nu_f)}$$

With this formulation, it is clear that α measures the mismatch in the plane tensile modulus across the interface. It can be noticed that α ranges from -1, when the film is extremely compliant to the substrate, to +1, when the film is extremely stiff compared to the substrate. When $\alpha = 0$, we have the perfect matching in the plane elastic moduli of the film and the substrate. On the other hand, β represents a measure of the mismatch in the in-plane bulk modulus, that is, in a plane strain condition, $\beta = 0$ if both materials are incompressible ($\nu_s = \nu_f = 0.5$). Another important consideration is that both parameters can be zero if no dissimilarity between the elastic properties of the materials is present.[26,36]

In-plane strain, the physical admissible values of α and β are restricted in a parallelogram enclosed by $\alpha = \pm 1$ and $\alpha - 4\beta = \pm 1$ in the (α, β) plane, as depicted in the plot in figure 20. The most common combinations of material pairs fall between $\beta = 0$ and $\beta = \alpha/4$.[26,37] In the following, we make an important assumption, that is, β is considered approximatively zero, simplifying all the consideration.

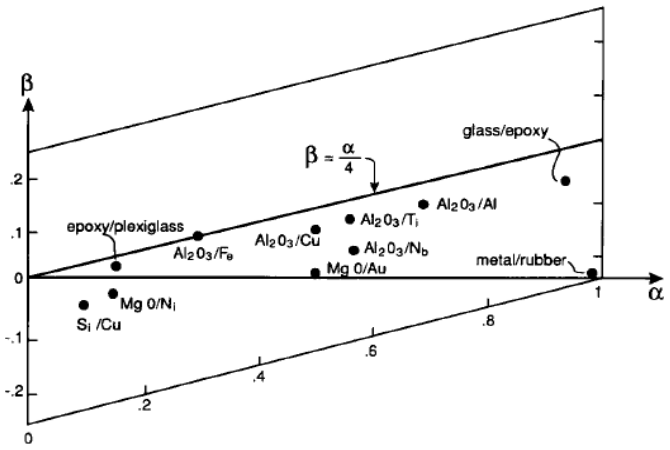

Figure 20 - Values of Dundurs parameters in plane strain for a selected combination of materials[26]

2.2.2 Mechanical properties of interfaces

We have seen that cracks in elastic, isotropic and homogeneous materials propagate mainly with pure mode I conditions; that is, when cracks will follow a path in which it is subjected only to an opening mode. The description of this type of fracture mode is given by the mode I stress intensity factor K_I.

On the contrary, an interface is a region of two joined materials with different mechanical properties. Since we are considering a bimaterial system, this implies an asymmetry in the moduli with respect to the interface which induces not only a fracture mode I, but also a mode II component of fracture. This is one of the main differences between interfacial fracture mechanics and fracture mechanics for isotropic homogeneous materials in which mode I toughness is relevant.[26,36]

For each material pair, a universal singular crack tip field exists at the crack tip belonging to the interface, and for plane problems, taking as the origin of the coordinate axes the crack tip, as shown in figure 18, the normal and shear stresses of the field acting on the interface at a distance r ahead of the tip can written as:[36]

$$\sigma_{xx} + i\sigma_{yx} = \frac{(K_1 + iK_2)r^{i\varepsilon}}{\sqrt{2\pi r}}$$

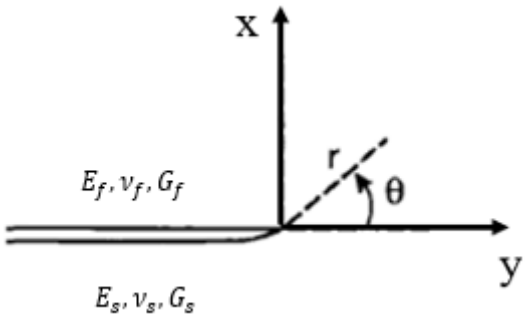

Figure 21 - System of polar coordinates at the crack tip[26]

The formulation of this stress field acting near the crack tip is written in a complex form where i is the imaginary number, while ε is called oscillation singularity index and depends on β as follows:

$$\varepsilon = \frac{1}{2\pi}\ln\left(\frac{1-\beta}{1+\beta}\right)$$

The energy release rate for crack propagation in the interface is similar to the energy release rate in isotropic and homogeneous material, but it takes into account the presence of elastic mismatch at the interface, and it is given by:

$$G = \frac{1-\beta^2}{E^*}(K_1^2 + K_2^2)$$

Where E^* is defined as:

$$E^* = \frac{1}{2}\left(\frac{1}{\bar{E}_f} + \frac{1}{\bar{E}_s}\right)$$

Now, the stress intensity factor is defined as a complex quantity of the form $K = K_1 + iK_2$, where K_1 and K_2 play a similar role to the conventional fracture mode I and mode II, but of course they cannot be interpreted as straightforward as opening and shearing opening.

If we analyse the formula of the stress field at the crack tip and the energy release rate, we can notice that if $\beta \neq 0$ (thus $\varepsilon \neq 0$), some complications in this theory appears, in particular the implementation of interfacial mechanics, so, it is reasonable making an approximation which is valid for our work, that is $\beta = 0$. If we assume this approximation, stress field and energy release rate can be treated simply, and K_1 and K_2 have conventional interpretations as K_I and K_{II} measuring the singularity of normal and shear stresses, respectively, on the interface ahead of the tip.

A measure of the relative amount of mode 2 concerning the mode 1 is given by mode-mixity phase angle Ψ as:[36]

$$\Psi = \tan^{-1}\left(\frac{K_2}{K_1}\right)$$

From an energetic point of view, we have seen that adhesion can have different interpretations (section 1.4.2), and we know that the more reliable adhesion measurement is given by the thermodynamic adhesion, which provides the actual work of adhesion W_A, depending on the bonding established between film and substrate and substrate contamination. Assuming that interface has its mechanical properties, fracture toughness for an interface could be associated, labelled as Γ_i. We can associate the fracture toughness for interface as equal to the true work of adhesion, that is $\Gamma_i = W_A$. However, this is not always true since adhesion measurements give us the practical work of adhesion. Indeed, the energy involved in the delamination process could be lost for every possible plastic dissipation in the film and in the substrate, and for interfacial friction. Hence, $W_{A,P}$, the practical work of adhesion, is:

$$W_{A,P} = W_A + U_f + U_s + U_{fr}$$

Where U_f and U_s are the losses of energy due to plastic dissipation in the film and substrate, respectively, and U_{fr} is the energy lost by friction.[38]

The amount of dissipation due to plasticity and friction is related to the mode-mixity angle and the figure 22 clearly describes this relation. We can see that if the only opening mode ultimately governs the fracture, that is $\Psi = 0°$ (mode I fracture toughness), the energy dissipation is less compared to the completely shearing mode fracture, $\Psi = 90°$ (mode II fracture mode). The interfacial fracture energy Γ_i is always larger than the thermodynamic work of adhesion W_A and it is monotonically increasing as Ψ increases, which is due to roughness-induced shielding and plastic dissipation. Roughness has a non-planarity effect on the local fracture resistance of interfaces because the contacting facets resist the motion of the crack surface due to friction.[39,40]

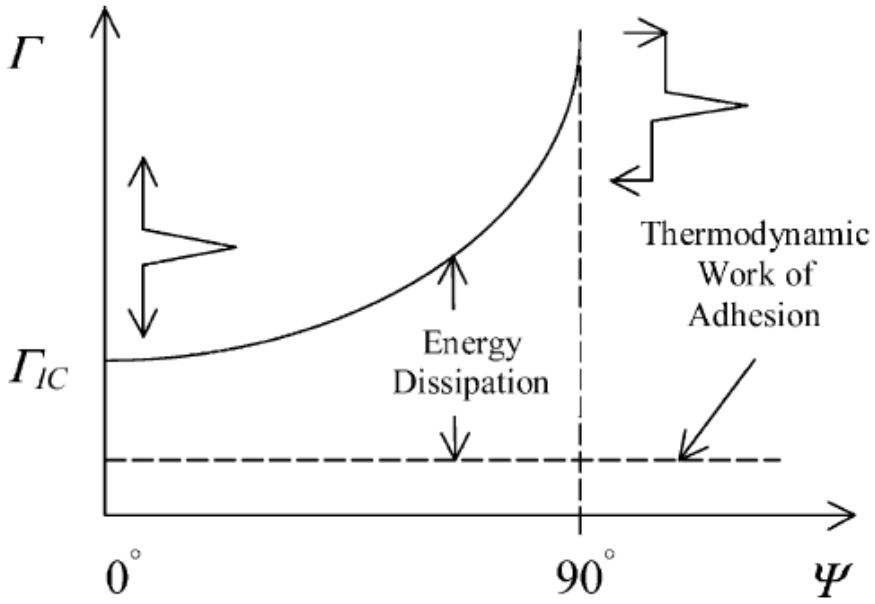

Figure 22 - Interfacial fracture energy as a function of the mode-mixity angle[38]

2.3 Crack propagation in film/coating systems

Dundurs parameters are crucial in developing of a quantitative theory concerning the formation of cracks into the film and its subsequent possible delamination from the substrate, since only two dimensionless mechanical properties are needed. As discussed previously, cracks are generated from defects into the material (inclusions, voids) or from boundaries and edges. Under certain conditions, cracks can propagate in an unstable way. Depending on the film/substrate materials and their mechanical properties, the crack may stop at the interface, penetrate the substrate, or bifurcate onto the interface, which is the primary source of thin film delamination, and, depending on where the crack propagates, the energy release rate must be higher than the related fracture resistance for the crack growth.[26,41] These three cases are depicted in figure 23. We will not consider the crack propagation penetrating the substrate because of the assumption that the interface and substrate are tough.[26]

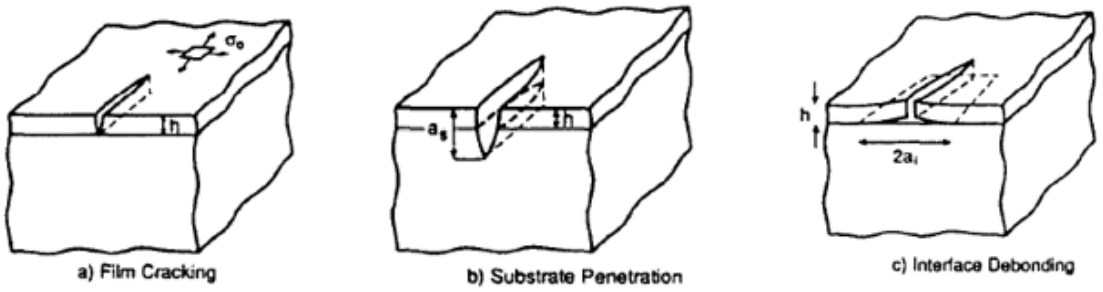

Figure 23 - Three types of crack propagation a) a channelling crack within the thin film, b) a channelling crack penetrating through the substrate and c) a channelling crack into the interface[41]

2.3.1 Crack propagation into the film material

We know that around each crack tip inside a homogeneous material exists a stress field, so, based on where the crack tip is, the stress field can change, and of course changes the fracture toughness. The general expression of the stress field σ_{ij} for $r \to 0$ like:[31]

$$\sigma_{ij} = \frac{K_I}{\sqrt{2\pi r}} f_{ij}^{I}(\theta) + \frac{K_{II}}{\sqrt{2\pi r}} f_{ij}^{II}(\theta) + \frac{K_{III}}{\sqrt{2\pi r}} f_{ij}^{III}(\theta)$$

Where r and θ are the polar coordinates centred at the crack tip, K_I, K_{II} and K_{III} are the stress intensity factors in mode I, II and III, respectively, and f_{ij} is an adimensional function of θ coordinate. We neglect mode III out-of-plane fracture because of plane condition. Mode I fields are symmetric to the crack line with $f_{xx}^{I} = 1$ and $f_{yx}^{I} = 0$ on $\theta = 0$, while the mode II fields are antisymmetric with $f_{xx}^{II} = 0$ and $f_{yx}^{II} = 1$ on $\theta = 0$. Based on these considerations, we get:[25,26]

$$\sigma_{xx} = \frac{K_I}{\sqrt{2\pi r}}$$

$$\sigma_{yx} = \frac{K_{II}}{\sqrt{2\pi r}}$$

If we consider a nucleated crack in the film, this could propagate in a three-dimensional way both towards the interface touching the substrate and laterally through the film, and these cases fall into the case of cohesive fracture mode, due to the fact that the crack propagates into a single material. A simplification of this mechanism is given by Beuth. In its work he divided the 3D problem into two elastic plane strain problems: the first one represents a given crack that propagates towards the interface with a perpendicular path, and the crack tip is inside the film, so the size of the crack is smaller than the film thickness (fig. 24a), the latter is the same crack, but its tip touches the interface (fig. 24b).[35]

Let's consider the first problem and suppose that the crack tip is into the film; that is, the crack length a is less than the film thickness h_f ($a < h_f$), as depicted in figure 24a, where material 1 stands for the coating/film, while material 2 stands for the substrate. In this situation, the stress singularity around the tip is inside material 1. Thus, this situation can be treated with the classical fracture mechanics problem, where the fracture toughness is related to mode I fracture. A critical assumption is that the stress is uniformly distributed along the film thickness.

If we take a coordinate reference system with the origin coincident to the crack tip, the x-axis along the applied stress and the y-axis along the through-thickness crack, then the stress intensity factor in mode I reads:[35]

$$K_I = F\left(\alpha, \beta, \frac{a}{h_f}\right)\sigma_0\sqrt{\pi h_f}$$

Where σ_0 is the applied stress, which is uniform along the crack length, while $F\left(\alpha, \beta, a/h_f\right)$ is a dimensionless quantity that depends on the two Dundurs parameters and the ratio between the actual crack length a and the thickness of the crack h_f.

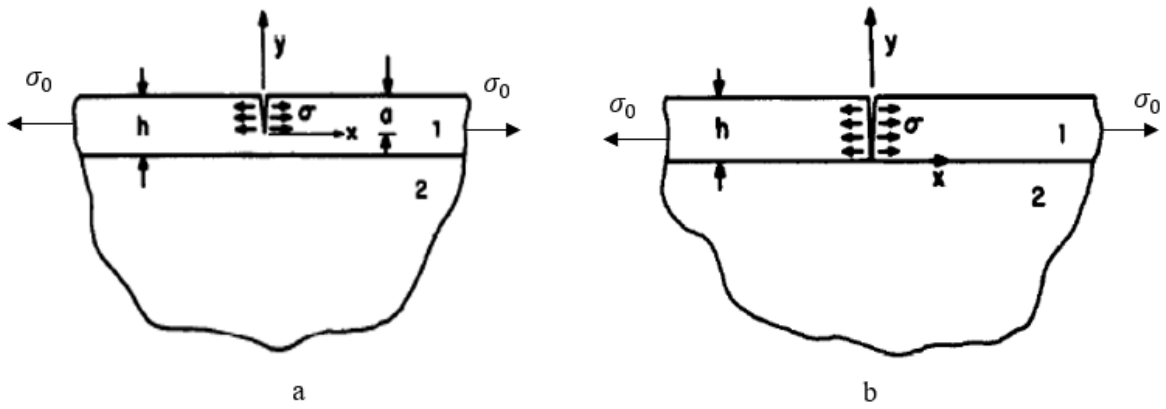

Figure 24 - a) Partially cracked film and b) the fully cracked film problems[35]

It is important to highlight that the fracture toughness depends not only on the film properties, but also on the substrate through the quantity F, which depends on the Dundurs parameters, although the crack is into the film material. The graphical and approximated formula for the dimensionless quantity F as a function of Dundurs parameters and the normalized crack length are reported in literature by Beuth.[35]

Two cases have to be analysed based on the Dundurs parameter α. Every material has its critical stress intensity factor, K_{IC}, which is the limit case above which cracks propagate unstably. Under the hypothesis of $\beta = 0$, if we consider a defect of a certain size a in a compliant film ($\alpha < 0$), a crack will never touch the interface for two reasons:

- K_{IC} is so large that no defects of a certain size can propagate towards the interface
- Given a certain K_{IC}, which is associated a critical $(a/h)_c$, if the crack has a dimension less than $(a/h)_c$, it will not propagate because $K_{IC} > K_I$, while, if the crack has a dimension more than $(a/h)_c$, the crack propagates until K_{IC} is reached, and then it will stop at a certain value of size without never reaching the interface

On the contrary, for films that are stiff relative to the substrate ($\alpha > 0$), K_I approaches infinity as a/h approaches 1. As a result, for a given flaw size in a stiff film, once K_{IC} is reached, the crack will propagate toward the interface, resulting in the fully cracked film, which is of interest

to us.[35] Concerning stiff substrate and complaint film, cracks tend easily to be attracted to the interface when we have a compliant substrate and stiff film.[41]

However, the crack tip is inside the film material ($a < h$), so we have considered so far surface cracks but if the crack tip approaches the interface, that is $a \to h$ or $a/h \to 1$, then, the evaluation of the stress intensity factor around the tip involves a different formulation, that is, instead of having the square root of r, we have the singularity exponent s, calculated using the Zak-Williams equation:[42]

$$\cos(s\pi) = 2\frac{\alpha - \beta}{1 - \beta}(1 - s)^2 - \frac{\alpha - \beta^2}{1 - \beta^2}$$

In this case, the stress intensity factor K_I is defined as:

$$K_I = f(\alpha, \beta)\sigma_0 \sqrt[s]{\pi h_f}$$

2.3.2 Through-film channelling cracks

Cracks can propagate not only towards the interface but also propagate in the third direction, along the width of the specimen (the so-called channelling cracks), as represented in figure 25, and this propagation is treated considering the steady-state energy release rate G_{SS}, which is the energy required to create new surfaces in a stationary condition. In this situation, cracks propagate, maintaining its shape as it advances. This stationary condition is reached when the crack length exceeds several film thicknesses considering it as independent on the crack length and the initial flaw size.[26,35]

This problem was firstly solved by Nakamura et al. for the case of a strongly compliant thin film bonded in a highly stiff substrate in a three-dimensional solution ($\alpha < 0$). They discovered that, in the absence of delamination, crack can channel the film in a steady state condition if the crack length is twice higher than the film thickness.[43] For a more compliant substrate to the film ($\alpha > 0$), a steady state energy release rate is reached when the crack length is significantly larger than the film thickness, more or less 20 times the film thickness. Moreover, also the

location of the crack can change the appearance of G_{SS}, if the crack is an edge crack or if it is a centre crack.[44] Definitely, we consider nucleated cracks which are very long with respect to the film thickness.

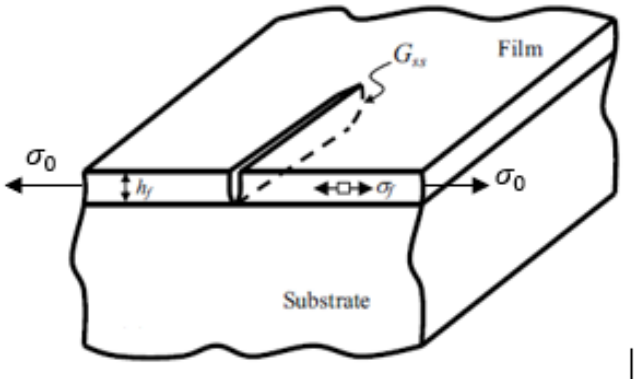

Figure 25 - Steady state channelling crack across the film[27]

At this stage, a dimensionless parameter is useful to introduce to describe better the evolution of a steady state crack propagation in coating materials. Hu and Evans given the description of this quantity. In their research, they proposed for an elastic film and substrate a critical non-dimension parameter Ω_c for the through-film channelling crack defined as:[45]

$$\Omega_C^f = \frac{\bar{E}_f \Gamma_f}{\sigma_0^2 h_f}$$

From which the critical fracture toughness for thin film Γ_f is:

$$\Gamma_f = \frac{\Omega_C^f \sigma_0^2 h_f}{\bar{E}_f}$$

Where Γ_f is the fracture toughness for the crack propagation into the film material in mode I condition, and it is related to the critical stress intensity factor K_{IC}^f through the Irwin relation:

$$K_{IC}^{f} = \sqrt{\bar{E}_f \Gamma_f}$$

In the ideal case where we consider an isolated crack in a purely elastic thin film, we can assume that $G_{SS} = \Gamma_f$. From this condition, the crack starts to propagate in a channelling mode. This non dimensional parameter is useful to create a fail-safe criterion, in order to prevent crack propagation, so the condition we want to achieve is when $G_{SS} < \Gamma_f$.[25]

Beuth derived the steady-state energy release rate G_{SS} for the 3D channelling crack for a thin film on a semi-infinite substrate with an elastic mismatch (fig. 25). The relation reads:

$$G_{SS} = \frac{\pi \sigma_0^2 h_f}{2\bar{E}_f} g(\alpha, \beta)$$

Where $g(\alpha, \beta)$ is a dimensionless quantity defined as:

$$g(\alpha, \beta) = \frac{\int_0^h \delta(y) dy}{\pi \frac{\sigma_0}{\bar{E}_f} h_f^2}$$

Where $\delta(y)$ is the crack opening displacement along the y-axis. We can notice that $g(\alpha, \beta)$ becomes constant (falling into the steady state condition) when the crack front remains constant.[35] Now, if we compare the steady state energy release rate G_{SS} derived by Beuth with the fracture toughness of thin film, the safety condition Ω_C^f reads:

$$\Omega_C^f = \frac{\pi g(\alpha, \beta)}{2}$$

2.3.3 Crack propagation along the interface – interfacial delamination

Supposing that the defect or flaw can propagate towards the interface and channel through the film, this crack can propagate penetrating the substrate or deflecting along the interface. We

will not consider the first case, focusing the attention on interface crack propagation. This situation is the driving force for possible delamination of thin films, so, in this case, we want to analyse the interfacial fracture toughness Γ_i. In order to have interfacial crack propagation, the interfacial toughness must be lower than the fracture toughness of the substrate.

Let's consider the figure 26, where we can see the channelling crack and interfacial delamination that occur simultaneously The energy release rate that we consider for this situation is the energy emanating due to the film detachment from the substrate G_D, while d is the delamination width.[27]

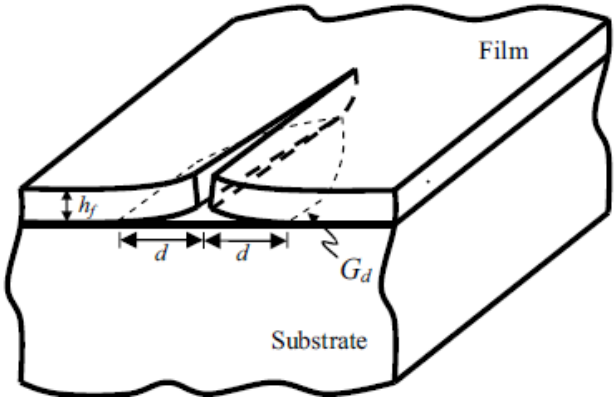

Figure 26 - Channelling crack and thin film delamination occurring at the same time[27]

The energy release rate for thin film delamination reads:

$$G_d = Z_d\left(\alpha, \beta, \frac{d}{h_f}\right)\frac{h_f\sigma_0^2}{\bar{E}_f}$$

Where Z_d is a nondimensional parameter that depends not only on Dundurs parameters α and β, but also on the ratio between the delamination width and the film thickness. It can be shown that for long delamination width ($d \gg h_f$), propagation reaches a steady state condition where $Z_d \to 0{,}5$, so:[27,41]

$$G_{ss}^d = \frac{h_f\sigma_0^2}{2\bar{E}_f}$$

On the contrary, if $d \ll h_f$ (case of the short crack), Z_d can be approximated with a power law, that is, $Z_d \sim \left(d/h_f\right)^{1-2s}$, where the solution of the Zak-Williams equation gives the coefficient s (section 2.3.1).[27,42]

The problem arises when considering the crack propagation along the interface as not purely fracture mode I, but a mixed mode fracture exists, and it has been highlighted that the interfacial fracture toughness Γ_i depends on mixity-mode phase angle Ψ (section 2.2.2). When $d \gg h_f$, it is shown that the mixity-mode angle reaches a stationary value, depending on the Dundurs parameters, so we consider the interfacial fracture toughness as only dependent on the steady state mixity-mode phase angle $\Gamma_i = \Gamma_i(\Psi_{ss})$. Based on this, the nondimensional parameter Z_d can be written as:[27]

$$Z_d\left(\alpha, \beta, \frac{d}{h_f}\right) = \frac{\bar{E}_f \Gamma_i(\Psi_{ss})}{h_f \sigma_0^2}$$

Knowing that $\Gamma_f = \Omega_C^f \sigma_0^2 h_f / \bar{E}_f$, we can rewrite Z_d as:

$$Z_d = \Omega_C^f \frac{\Gamma_i(\Psi_{ss})}{\Gamma_f}$$

But, in a steady state condition, when $d \gg h_f$, Z_d is independent on the crack length and assumes the value of $0{,}5$, so, the condition for determining Γ_i in mode I is:[41]

$$\Gamma_i = \frac{\Gamma_f}{2\Omega_C^f}$$

2.3.4 The role of ductile substrates

We should implement the study of crack nucleation and propagation, since we have considered so far that film and substrate have only a linear elastic behaviour, but, if the external applied stress exceeds the yield strength σ_y of one or both materials, then, that material falls into the plastic region, in which, no linearity between stress and strain is present. Now, we want to

analyse the role of the substrate plasticity in crack propagation. In section 2.1.1 it is highlighted that there are some constitutive equations useful to model the plastic region in the stress-strain curve, and two are very commonly used:

- Linear elastic-perfectly plastic behaviour, where, once the yield strength σ_y is reached, this value is considered constant for subsequent deformation, and it is the easiest model to understand plastic behaviour:

$$\begin{cases} \sigma = E\varepsilon & \varepsilon < \dfrac{\sigma_y}{E} \\ \sigma = \sigma_y & \varepsilon \geq \dfrac{\sigma_y}{E} \end{cases}$$

- The Ramberg-Osgood equation is mainly used for materials presenting hardening behaviour when these materials are subjected to plastic deformation. The hardening phenomenon is common in steel. The total strain ε is decoupled in two different values: the elastic strain ε_e component, which follows the linear elastic behaviour again, and the plastic strain ε_p component, which follows a different relation:

$$\sigma = H\varepsilon_P^{1/n}$$

Where H and n are two material constants describing the material strain hardening. The equation describing it is:[31]

$$\varepsilon = \varepsilon_e + \varepsilon_p = \frac{\sigma}{E} + \left(\frac{\sigma}{H}\right)^n = \frac{\sigma}{E} + K\left(\frac{\sigma}{E}\right)^n$$

Where $K = \left(\frac{H}{E}\right)^n$. If $n = 1$, the material is completely dominated by elastic behaviour, on the contrary, if $n \to \infty$, the material has an elastic-perfectly plastic behaviour. Another formulation of the Ramberg-Osgood is given by substituting $E = \sigma_y/\varepsilon_y$:[46]

$$\frac{\varepsilon}{\varepsilon_y} = \frac{\sigma}{\sigma_y} + \alpha\left(\frac{\sigma}{\sigma_y}\right)^n$$

Extended the research of crack propagation theory including substrate plasticity is of paramount importance, since the material's yielding has detrimental effects on crack opening displacement $\delta(y)$. We know that if the crack opening displacement increases, this is the driving force for further channelling propagation, because it is related to the dimensionless parameter $g(\alpha, \beta)$, which is presented in the research by Beuth.[35] An extension of his work, in which film and substrate were supposed to be isotropic and linear elastic, Beuth et al. proposed a further modification of the previous study including the role of substrate ductility. They supposed that the film has a brittle behaviour, so it obeys the linear constitutive equation between stress and strain, while substrate obeys a purely Ramberg-Osgood constitutive equation. The model is based on the analysis of two parameters: the former is related to the strain hardening exponent n, the latter is related to the yield strength σ_y, in particular σ_0/σ_y. Again, a steady state energy release rate for channelling crack in a coating can be written as:[46]

$$G_{SS} = \frac{\pi \sigma_0^2 h_f}{2\bar{E}_f} g\left(\alpha, \beta, \frac{\sigma_0}{\sigma_y}, n\right)$$

Now, the non-dimensional parameter g is not only a function of Dundurs parameters, but also on the parameters characterizing the ductility of the substrate. As done for the case of elastic problem, if channelling crack propagation occurs, we must have that $G_{SS} > \Gamma_C$, thus, it is required a lower possible value of G_{SS}. This can be obtained by reducing the applied stress and the film thickness. At the same time, we have to analyse the role of the dimensionless quantity g, which has to be lowered. It is found that g can be lowered not only by having a stiff substrate and compliant film ($\alpha < 0$), as it was shown previously, but also by increasing the yield strength of the substrate σ_y and having a substrate material with more strain hardening (higher value of the strain hardening exponent n).[46]

In order to formalize the non-dimensional quantity g using measurable quantities, it is helpful to introduce the concept of shear lag approximation, in which, near the interface, we consider the substrate as slipping material. In contrast, the remaining part of the substrate behaves again elastically. If we consider that along the interface a sliding between film and substrate occurs, the presence of shear stresses caused by the yielding phenomenon appears, so the steady state

energy release rate G_{SS} must take into account this constant shear stress τ_0, related to the yield strength σ_y as $\sigma_y = \sqrt{3}\tau_0$, acting on the interface.

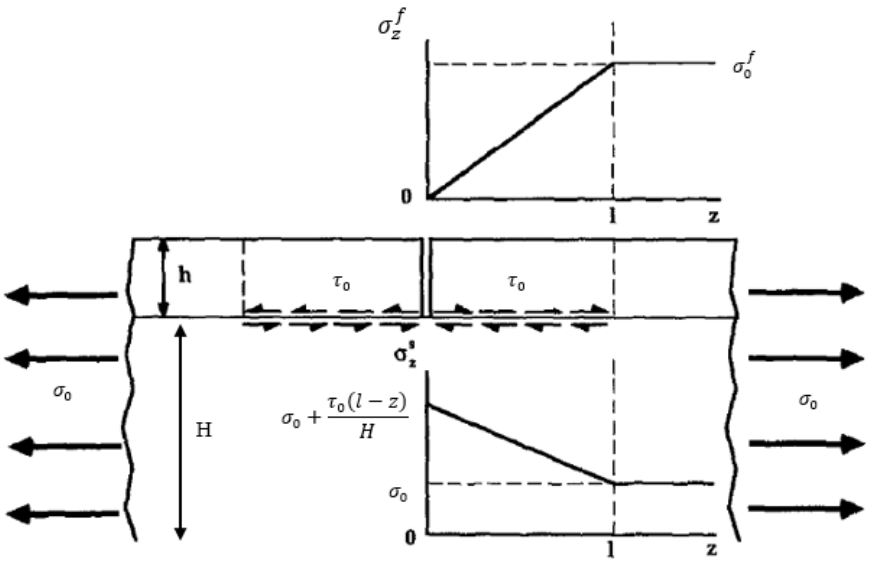

Figure 27 - Schematic representation of the shear lag approximation with interface modelled as plastic[45]

An important parameter to be defined is the slip length l as the distance from the crack above which the stress in the film could be considered constant, assuming the value of the applied stress σ_0, is:[45]

$$l = \frac{\sigma_0}{\tau_0} h_f = \frac{\sqrt{3}\sigma_0}{\sigma_y} h_f$$

Avoiding the computations of deriving G_{SS}, this can be finally expressed as:[45]

$$G_{SS} = \frac{\sigma_0^2 h_f}{\bar{E}_f} \left[\frac{\sigma_0}{\sqrt{3}\sigma_y} + \frac{\pi g(\alpha, \beta)}{2} \right]$$

We can notice from this equation that the steady-state energy release rate G_{SS} is spitted into two contributes: one is related to the elastic solution, and one from the plasticity of the substrate. If the applied stress σ_0 is less than the yield strength σ_y, then, the plastic term drops to zero, leading to the previous elastic solution of G_{SS}. The steady state energy release rate depends on the elastic solution, previously derived, by considering the dimensionless parameter g, and on the ratio between the applied stress σ_0 and the yield strength σ_y, and higher values of σ_y corresponds to lower values of G_{SS}, thus, the tendency to enhance the channelling crack propagation is higher if the yield strength decreases. This can also be seen analysing the slip length, because a lower value of shear strength corresponds a higher value of l, which causes an increase in the crack opening displacement due to the extension of the slipping zone.

A final consideration is related to the delamination of coatings under plastic deformation of the substrate. Again, it could be possible having thin film decohesion from the substrate if the fracture toughness is lower than the fracture toughness of the substrate, but, in the case of yielding, the decohesion occurs only if the yielding strength of the substrate is higher.

2.4 Multiple crack propagation in thin films

Up to now, a theory has been derived for an isolated crack propagating in a thin film, and it is well- known that a crack grows and propagates if defects inside the film or edges are present. Since we are considering a bimaterial composite, the propagation must obey the mismatch between film and substrate's elastic mechanical parameters, which is summarized into the Dundurs parameters α and β. For the sake of simplicity, it is assumed that $\beta = 0$.

A crack can propagate or not toward the interface depending on these parameters. We have found that for $\alpha < 0$ (substrate stiffer than the film), crack cannot propagate at all towards the interface; on the contrary, for $\alpha > 0$ (substrate more compliant than the film), once the critical fracture toughness of coating is overcome for a particular size of the crack, this propagates touching the interface. At the same time, this crack can propagate through the width of the film channelling it. In this case, a steady state energy release rate is an important quantity for defining this phenomenon, and it is reached when the propagation length is much more than the

film thickness. Then, once the crack tip touches the interface, two situations can occur: crack can penetrate the substrate, or crack can deflect along the interface. We have considered the latter situation, because the fracture toughness of the substrate is higher than the fracture toughness of the interface. Also in this case, a steady state crack propagation along the interface is reached when the crack size is much more than the film thickness. Finally, we have considered the effect of substrate ductility, in particular the yield strength of the substrate, on crack propagation. It is found that the yield strength enhances the probability of having channelling cracks into the film, and at the same time, the lower is this value, the higher is the steady state energy release rate.

2.4.1 General trend of multiple channelling cracks

Under uniaxial tensile stress, film that covers the substrate first starts cracking with random crack formation along the length of the coating. These can be formed by the presence of defects inside the film (centre cracks) or by its boundaries (edge cracks).[44] These cracks tend to propagate channelling along the layer's width perpendicularly to the external load. Increasing again the applied stress, these cracks formed in a statistical distribution with no evident periodicity start to interact with each other forming new cracks that now, at a certain point, form a very high regular distribution with a certain crack spacing. Finally, this crack spacing reaches a stationary value, below which no further cracks can be formed between two cracks, and in this case a crack film saturation is achieved.

The interaction between two cracks is a very crucial parameter since above a certain value of the distance between two of them, these cannot interact, and random cracks continue to form. Touless reported in his research the fact that, once the cracks are developed, the crack spacing should not be more than eight times the film thickness for having interaction in a film-substrate composite with identical elastic moduli , but other studies show that this condition is not true at all, that is, this value should be more than eight times the film thickness for two reasons: the first reason is related to a statistical distribution of defects, the second one is related to the critical shear stress at the interface due to substrate ductility.[32]

Two types of crack patterns can be found: simultaneous advance crack pattern, in which every crack is advancing with the same length along the width of the film, and sequential advance crack pattern, in which a different crack pattern grows with a length equal for each growing crack, but different from the previous pattern. These two patterns are depicted in figure 28.[47]

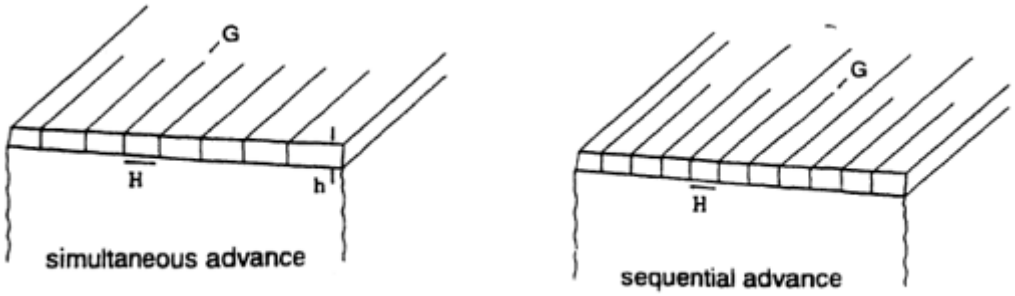

Figure 28 - Simultaneous advance (left) and sequential advance (right) crack patterns[47]

Let us analyse the case of a simultaneous advance crack pattern, restricting our analysis to the simple case of a homogeneous elastic system. We can suppose that there exists a steady state energy release rate for creating multiple cracks with periodicity of distance H and same width (of course, this is an approximation, the real situation follows a statistical distribution of cracks that are not all equally spaced at distance H). In this case, G_{SS} is:[26,47]

$$G_{SS} = f_m\left(\alpha, \beta, \frac{h_f}{H}\right)\frac{h_f \sigma_0^2}{\bar{E}_f}$$

Where f_m is a nondimensional parameter depending on the elastic mismatch and the ratio between film thickness and crack spacing. We can notice that this formulation is identical to the case of an isolated channelling crack derived by Beuth, in which $f_m = g$ if the crack spacing between two cracks H is large (the two cracks behave as isolated ones).[26]

Our scope is to determine a specific formulation of f_m depending on measurable quantities. Xia et al. derived in their work the energy release rate for a multiple crack pattern with crack spacing equal to H as:[47]

$$G_{SS} = \frac{h_f \sigma_0^2}{2\bar{E}_f} \pi g(\alpha, \beta) \tanh\left[\frac{H}{\pi g(\alpha, \beta) h_f}\right] = \frac{l\sigma_0^2}{\bar{E}_f} \tanh\left(\frac{H}{2l}\right)$$

Where, for a compactness formulation, the reference length l is defined as:

$$l = \frac{1}{2} \pi g(\alpha, \beta) h_f$$

If $H \gg l$, we notice that the steady state energy release rate for multiple cracks collapses to the steady state for isolated cracks, and this occurs when h_f is relatively low, or, at the same time, when $g(\alpha, \beta)$ is low, and this implies $\alpha < 0$, that is, stiff substrates and compliant films. From another point of view, if $\alpha < 0$, cracks have to interact if their distance is relatively small, and vice versa.

Let us suppose now that a set of middle cracks between two infinite cracks starts to propagate, idealizing a sequential advance crack pattern. The energy release rate needed to propagate each semi-infinite crack is again derived by Xia et al[47] and following by Yin et al.[48]:

$$G_{SS} = \frac{l\sigma_0^2}{\bar{E}_f} \left[2\tanh\left(\frac{H}{2l}\right) - \tanh\left(\frac{H}{l}\right)\right]$$

Where H represents the distance between the infinite crack and the growing middle crack, as represented in figure 29. If we equalize $G_{SS} = \Gamma_f$, then, we can find the level of stress at which this new crack pattern can be formed.

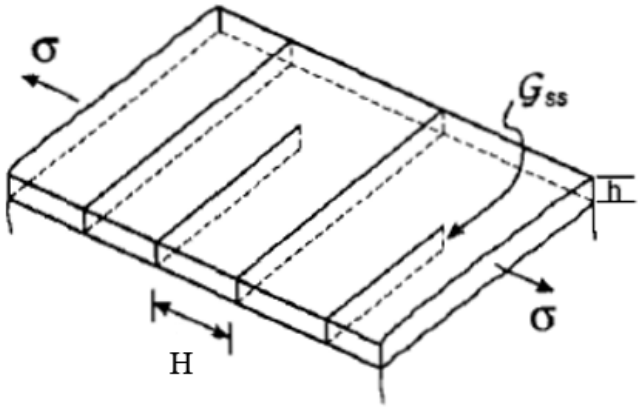

Figure 29 - Representation of multiple cracks with crack spacing H[26]

2.4.2 Interfacial shear strength

We have seen that under specific stress and material conditions, cracks propagate along the width of the film with the crack tip touching the interface. If another crack can be formed randomly, it can interact with the first one if their distance is below at a certain critical size. If the distance between these two cracks is larger than this critical one, another crack can be formed randomly in between, on the contrary, usually, the growing crack propagate inside the two cracks, usually in the middle, where high values of in-plane stress are present.[49]

Let us consider two cracks A and B separated by a distance H that are formed into an elastic thin film, which, in turns, is covering a ductile substrate, as depicted in the figure 30. From section 2.3.4, we know that a ductile substrate has an important effect on crack propagation since applied stress higher than the yield strength can generate tangential (shear) stresses along the interface, creating a sort of slipping zone. This is represented by τ, which is the shear stress that acts along the interface and it represents the ideal shear strength of the bonds across the interface, while σ is the in-plane stress into the film, which is constant along the thickness of the film, but not along the crack spacing H, because it depends on the shear stress τ through the stress balance equilibrium for free body diagram:[50]

$$\sigma(x) = \frac{1}{h_f}\int_0^x \tau(x)dx$$

This hypothesis is consistent by searching into the work of Chen et al.[49], reported at the end of the section.

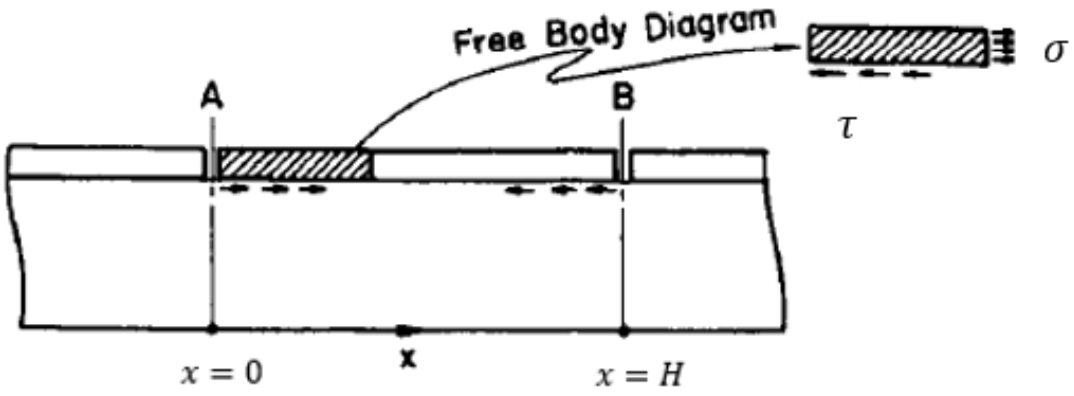

Figure 30 - Body diagram of two film cracks A and B[50]

From this equality, it is important to know what the shear stress function is in order to recover the stress that acts into the slice of film between the two cracks A and B. Agrawal et al. proposed for their research a sinusoidal function for the shear stress, that is zero at the crack edges ($x = 0$ and $x = H$), then reaches a maximum τ_0 (positive on the left and negative on the right), and finally drops again to zero at a distance $\lambda_0/2$ and $H - \lambda_0/2$. In the middle between $\lambda_0/2$ and $H - \lambda_0/2$, the shear stress is zero.

Computing the integral for the balance equilibrium provides the stress state that acts along the length of the film from A to B, and it exists a maximum of tensile stress into an interval of x values from $\lambda_0/2$ and $H - \lambda_0/2$ which is constant, that is:

$$\sigma(x) = \sigma_0 = \frac{\lambda_0 \tau_0}{\pi h_f}$$

Since the stress is maximum into this interval, new cracks can be formed inside it, and, of course, the formation of a new crack changes the stress distribution, so two situations must be analysed. If the crack is formed at the position $x = \lambda_0/2$, this situation implies the minimum crack spacing, which is equal to $\lambda_0/2$, and in this situation, the maximum shear stress formed in this minimum slice of the film is lower than τ_0. The second case that has to be considered is when the two adjacent cracks are distant λ_0, which is the maximum distance that can be obtained starting from two cracks at a distance H. Starting from two cracks at position A and B, a new crack is formed with a distance from A ranging from $\lambda_0/2$ to λ_0, thus, according to Agrawal et al. the set of transverse cracks has a statistical distribution of distances that should differ by a factor of two. Knowing the value of crack spacing λ_0, the stress σ_0 that provokes the fracture of the film; we can calculate the ultimate shear strength that acts on the interface:[50]

$$\tau_0 = \frac{\sigma_0 \pi h_f}{\lambda_0}$$

A modified equation of the previous one for the shear stress is given again by Agrawal et al. in which it considers an average value of crack spacings, that is:[51]

$$\tau_0 = \frac{\sigma_0 \pi h_f}{1{,}5\lambda_0}$$

The problem of this formulation proposed by Agrawal et al. is that the interfacial shear strength is zero near the two cracks using a full sine wave function. However, other researchers proposed another type of approximation, in which the shear strength has its maximum at the ends of the crack segment and zero in the middle. In their research, Chen et al. proposed a new formulation for the interfacial shear strength using as a model a quarter segment of an ellipse, and avoiding the calculations, the result is:[49]

$$\tau_0 = \frac{4\sigma_0 h_f}{(\pi + 4)\lambda_0}$$

Finally, a comment about the in-plane stress along the segment between two channelling cracks. In the research conducted by Chen et al., they discovered that narrower is the spacing between two channelling cracks, lower is the value of the maximum in-plane stress acting on the film, and further cracks develop in the middle of the segment. Consequently, the in-plane stress will not be sufficient for further channelling crack in the middle. This situation is described in the figure 31 extrapolated from their work, which describes a TiN coating on 304 SS substrate system.[49]

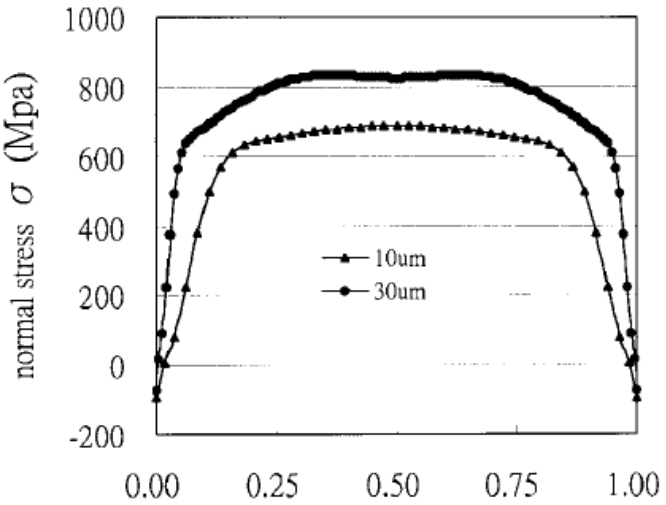

Figure 31 - Distribution of the in-plane stress in the film for two different crack spacings[49]

Moreover, the in-plane stress has been considered uniform along the cross-section of the coating, but, for thicker film this statement is not true at all. In this case, a finite element analysis (FEA) conducted by Wang et al. describes the effect of coating thickness. Two graphs in picture 32 represent the same coating-substrate system, but with different film thickness, where 32a refers to $1.8\,\mu m$ film thickness, while 32b refers to $18\,\mu m$ film thickness, one order of magnitude higher than the first one. The x-axis represents the semi-cracked segment of $22.5\,\mu m$ (the entire cracked segment between two channelling cracks is $45\,\mu m$), where $x = 22.5\,\mu m$ represents the segment edge. Colours represent the depth along the thickness from the interface (for example, in the plot 32a, the red-dotted curve represents the in-plane stresses distributed along the semi-cracked film at $0.45\,\mu m$ above the interface). From the graph 28a the in-plane

stress distribution along the x-axis is quite uniform along the thickness except near the edge, where the stress decreases, going to zero; on the contrary, for thicker films, the stress values are different and depends on the thickness, and surprisingly on the film surface compressive stresses arise ($x = 15.5\ \mu m$ and $17.5\ \mu m$ in plot 32b).[52]

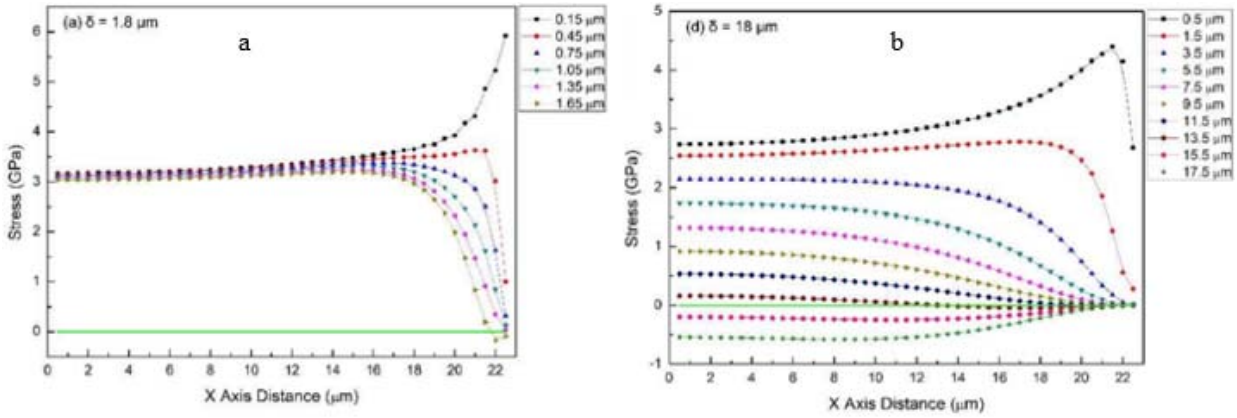

Figure 32 - In-plane stress distribution function of the semi-cracked film segment for a) 1.8μm and b) 18 μm film thickness[52]

Chapter 3 – Case study of Al_2O_3-PLD thin film

3.1 Introduction

An in-depth and exhaustive research of the material's physical-chemical, mechanical, optical, and thermal characteristics has allowed man to select them so that they can be suitable for specific applications. The deposition of thin films is an essential application in the field of material science, as reducing matter by one dimension allows for varying those properties that could not be had in three-dimensional solids. The reduction of one dimension implies the reduction of the film thickness; in fact, depositing a protective layer with smaller thicknesses provides more adherence onto a component.

One of the fields on which this thesis is based on is the research of suitable materials to deposit in the form of thin films and cover the underlying substrate from external agents that can cause its degradation, such as corrosion. Corrosion, therefore, is a chemical-physical process that leads materials to slowly wear out and deteriorate, precisely because of the environment in which they are immersed. A classic example of corrosion is that of iron in contact with an aqueous and oxidizing environment which leads it to become iron oxide, commonly called rust. Thinking about iron, or more precisely steel, this material is strongly used in a wide range of applications, however, it is easily perishable if it is constantly exposed to the external environment, and this degradation causes a drastic drop in the mechanical properties and possible structural damages and collapses.

A solution that engineers make use of on a large scale is precisely that of covering the material to be protected with thin films. Many solutions for thin film production are available in the literature. Two examples among these are thin films generated starting by the chemical composition of the material to be protected (for example austenitic steels, inside which there is a percentage of chromium, useful to form a stable chromium oxide film through oxidation) or through deposition techniques of a substance suitable for specific environmental conditions. The latter solution will be analyzed in detail through the study of a specific case of corrosion,

and specifically it will be important to consider strong and hard thin film as protective coatings to protect materials from any interaction with corrosive environments.

3.2 Nuclear reactor protection against heavy liquid metal corrosion

In the introduction of this chapter, it is focused on the attention to the problem of corrosion, in particular corrosion of steels caused by oxygen dissolved in water environment, now, a more specific case is analysed in details in the present work, that is the corrosion caused by heavy liquid metals (HLMs), which are specific substances, candidate as heat transport fluids in advance nuclear systems, due to their favourable thermo-physical and neutronic properties.[2,53]

Over the years nuclear reactors have become more and more efficient and probably generation IV nuclear reactors will be available not earlier than 2030. The most important features of this new class of reactors are concerning safety, waste, and efficiency. Among this generation, it is worth mentioning the Lead Fast Reactors (LFRs), which use as cooling material lead or lead alloys, knowing as LBE, specifically due to their no chemical reactivity in wet and oxidizing environments, high boiling temperature and high thermal properties. However, the major challenge in this regard is to find suitable materials for realizing reactors able to withstand the HLM corrosion in very severe environments, more specifically against LBE.[10]

Nuclear reactors are mainly made of steel or austenitic steel which suffer the high temperature HLM corrosion, and radiation damage. For such problems protective solutions must be considered. Several solutions have been tried for finding a good compromise in terms of film stability, such as density, porosity, and defects, adhesivity onto specific substrate and surface morphology, for example, growing a chromium oxide thin film by passivation of stainless steel, but this is not suitable for very high temperature operations (above 500 °C). Moreover, a higher concentration of oxygen accelerates the corrosion depth resulting in fast degradation of steel; on the contrary, a lower value of oxygen favours the dissolution of the structure by LBE since no stable oxide film can be grown.[2,54]

Using ceramic materials seems to be a good solution for their chemical inertness for higher temperature applications, nevertheless they present some drawbacks, such as brittleness, poor adhesive strength, and micro-cracks, that under exposure to a very severe environment could be deleterious to the structure below the ceramic film. In a research conducted by Ferrè et al. it was found that amorphous alumina thin film grown by PLD has excellent mechanical properties, similar to metals, good wear resistance and strong interfacial bonding. They compared an uncoated and PLD-alumina coated substrate steel under the same corrosive environment and time exposure. They noticed that the steel component under the coating was protected from lead.[2] Details of this PLD-alumina coating will be analysed in the following section.

3.3 Review of mechanical properties of alumina

3.3.1 Bulk alumina Al_2O_3

In this section, details for what concerns aluminum oxide Al_2O_3 (namely also as alumina or corundum) will be treated specifically. This oxide has some peculiar characteristics when it is deposited in thin films. However, before describing these critical features, we need to have a quick overview of the properties in the bulk form.

Among the different categories of materials, we know so far, we can find ceramic materials, characterized by a predominantly ionic crystalline structure, a particular bond between atoms that makes ceramics particularly hard with a high melting temperature. Alumina is considered the material under this study. It is formed by a metal, aluminum, and a non-metal, oxygen. Being more electronegative, oxygen tends to tear an electron from aluminum, which is instead more electropositive, that is, it easily yields an electron. Consequently, this unidirectional exchange of electrons favors the formation of stable charges, anions and cations, which interact strongly to create stable bonds through coulombic bonding forces, the keystone for having hardness and brittleness ceramic materials. The picture below describes the formation of sodium chloride (NaCl) as an example, but the situation could equally represent the formation of aluminum oxide.

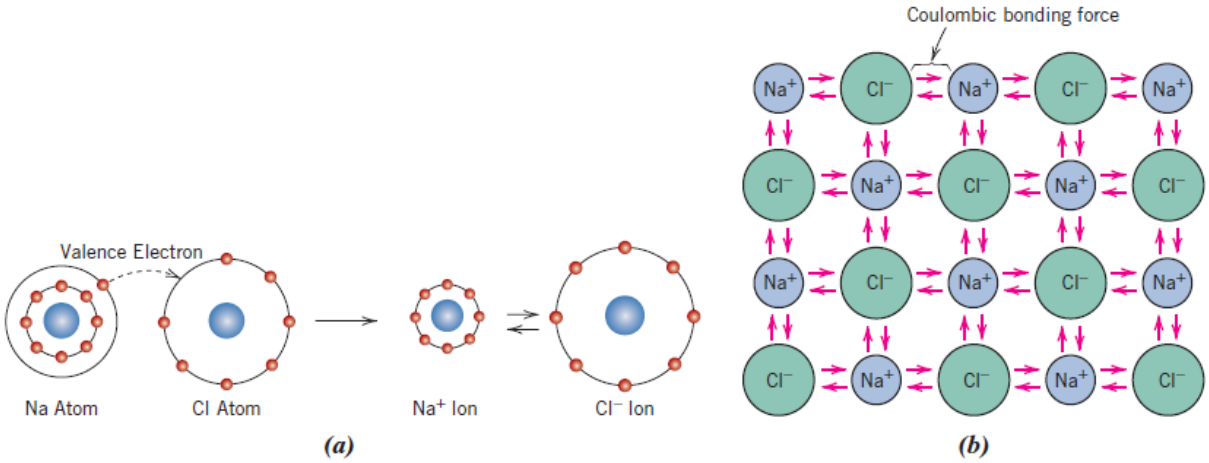

Figure 33 - Schematic representation of the crystalline lattice formation of NaCl[28]

Alumina is a polymorphic material so different crystalline structures for the same material could be observed; in particular, the most important ones are α, θ, and γ. However, the attention is focused mainly on the α-phase, which is thermodynamically stable up to its melting temperature of about 2050 °C. Nevertheless, below 1050 °C, alumina could appear in metastable phases mainly as θ and γ, and this circumstance complicates a lot the possibility of growing α-phase alumina thin film at lower temperatures. The α-phase crystalline structure is quite complicated, in fact, the Bravais lattice can be simplified as a hexagonal closed-packed (HCP) structure of oxygen anions, with 2/3 of the octahedral interstices filled with aluminum cations. The following table (fig. 34) extracted from the literature highlights critically the main transformations from mineral structures towards metastable phases and sequential steps for α-alumina.[55]

For engineering application, polycrystalline alumina is usually realized by hot-pressing synthesized powder at high temperature, and thus lower density and higher percentage of porosity must be taken into account. Alumina can be divided in grades, depending on the purity level of the alumina itself, and, of course, different thermal and mechanical properties can be obtained. Different grades are obtained considering the level of impurities present into the aluminum oxide and sometimes these impurities can be used as alloying elements with the scope of being sintering aids.[56]

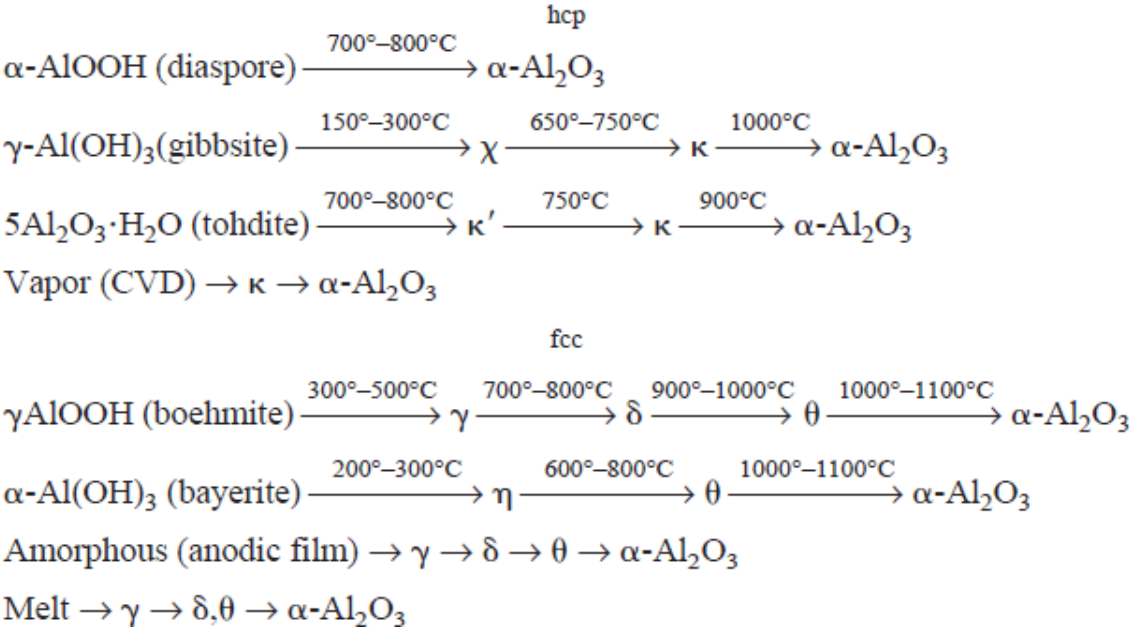

Figure 34 - Common transformation processes producing metastable alumina structures and α-alumina[55]

Since alumina is an oxide, thus with the presence of chemical bonds which are prevalently ionic, it presents the commonly mechanical properties of ionic materials, that is, hardness, brittleness, insulating, inertness, and transparent. Some values of the density and elastic modulus are reported in literature, in general, acceptable values for density are in the range of $3980 - 3990\ kg/m^3$, while for Young modulus values of this mechanical properties are very similar for all class of oxide materials, in the range of 400 to 440 GPa. Considering 99.9% purity of alumina, values of elastic modulus, Poisson ratio and stress intensity factor are $380\ GPa$, 0.22, and $4.2 - 5.9\ MPa\sqrt{m}$, respectively.[28,57,58]

3.3.2 Alumina thin film Al_2O_3 grown by PLD

Ceramic materials, particularly aluminum oxide, fall into the category of hard coatings. They are particularly useful in applications involving structural parts under abrasive and erosive environments, also at high temperatures. Moreover, their chemical inertness makes them suitable for corrosion protection. One main drawback is related to the higher stresses induced in the coating when it is deposited onto a relatively soft substrates, like steel, when it is externally loaded. Moreover, also the internal stresses must be considered when the deposition temperature is higher than the room temperature, but sometimes compressive stresses are beneficial.[59]

At this stage, it is essential to compare ceramic thin film deposition techniques in order to achieve coatings with well prescribed characteristics. Pulsed laser deposition seems to be a good candidate for this scope. As highlighted in chapter one describing various deposition techniques, PLD is suitable for depositing ceramic coatings since it can produce stoichiometric multicomponent films by using laser beam and depositing without the employment of heated substrate. The laser beam impinges onto a target, source of the material that we want to grow, and in the case of ceramic materials, these targets are realized by stoichiometric bulk sintered ceramics.[3]

Many studies have been done in this direction. As previously introduced, Ferrè et al. proposed their research of PLD-alumina thin film for nuclear reactor protection against severe environments like HLMs.[2] The aim of their research is to find a suitable solution for this issue, and hard, compact, and dense alumina film deposited using PLD seems to be the best solution. In order to achieve the solution, it is required to control PLD process parameters, such as partial pressure into the chamber, substrate-to-target distance, laser fluence, and so on. They found that by tuning the oxygen partial pressure into the deposition chamber, a compact homogeneous coating can be achieved with an oxygen partial pressure of $0.5\ Pa$, whereas for partial pressure above $5\ Pa$ the structure of the film becomes columnar and porous. Figure 35, extrapolated from the work done by Di Fonzo et al., represents the different microstructures of alumina deposited at different oxygen partial pressure. It is worth highlighting that different morphologies have a strong impact on the mechanical properties of the specific coating, in fact

increasing the oxygen pressure corresponds to a decrease in the density of the film, in the hardness and the reduced modulus.[60]

In this regard, a deep characterization of the mechanical properties and the microstructure of alumina thin film grown by PLD has been done by Ferrè et al. investigating that coating onto silicon and stainless-steel substrate at room temperature. Combining three different techniques, such as ellipsometry, Brillouin spectroscopy, and nanoindentation, they were able to extrapolate important mechanical quantities such as elastic modulus, Poisson ratio, shear modulus, and hardness. These values are reported in association of the uncertainty related to the measures of the alumina coating deposited at room temperature, and they will be used for the experimental measurements for the present work:[61]

- Elastic modulus E: $195.4 \pm 8.7\ GPa$
- Poisson ratio ν: 0.294 ± 0.021
- Shear modulus G: $75.5 \pm 4.3\ GPa$
- Hardness H: $10.3 \pm 1\ GPa$

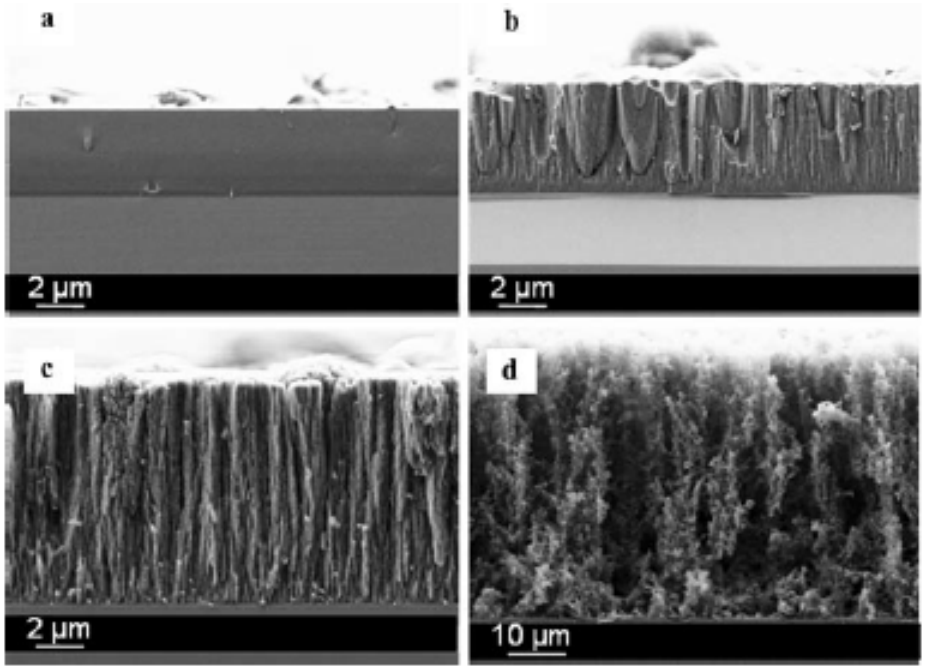

Figure 35 - Different morphologies of alumina thin film grown at a) 0.5 Pa, b) 5 Pa, c) 25 Pa, and d) 100 Pa at a fixed target-to-substrate position[60]

It is evident from the first two quantities, i.e., Young modulus and Poisson ratio, that thin film alumina has different mechanical properties deviating from the bulk ones, since oxides have always brittle behaviour, instead these values are quite peculiar of materials that have a ductile behaviour. This is something exceptional for what concern ceramic materials like oxide glasses at room temperature, in fact it is demonstrated that amorphous alumina thin film can deform permanently by plastic deformation reaching also high elongations without thermal activation, and this deformation can be related through the concept of diffusion mechanism. To state this experimental evidence, an indentation test has been used in order to permanently deform alumina coating.[62]

From a microscopical and morphological point of view, imaging is carried out again from Ferré et al. showing a peculiar characteristic of this deposition technique, that is, alumina thin film has an amorphous matrix structure in which 2-5 nm nanoparticles of crystalline α-phase alumina are dispersed into the amorphous structure. Figure 36 shows a TEM image of the alumina microstructure.[61]

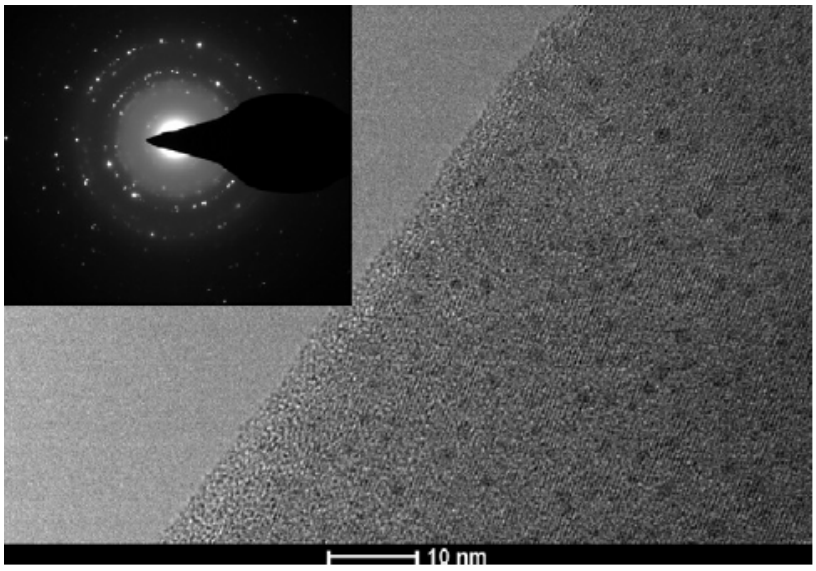

Figure 36 - TEM image representing an alumina coating of nanocrystalline phases (dark spots) embedded in an amorphous matrix[61]

3.4 Destructive adhesion measurements

Nowadays, adhesion measurements are performed mainly by destructive measurement techniques, in which the sample modifies irreversible. In mechanical methods adhesion is measured by applying a force to the film/substrate system, causing a stress at the interface which should detach the coating if the stress increases above a critical value. This stress at which film detaches from the substrate is taken as an experimental value of the measured adhesion. Two types of measures can be performed: the adhesion strength measurements and the interfacial toughness measurement. Both are influenced by the substrate preparation, substrate temperature, coating technique, and the residual pressure in the chamber.[20]

The detachment of the film is not the only condition that can happen, in fact the failure of the film/substrate system could be in the interface (that is the situation we want to analyse), in the interphase, or in bulk (called as cohesive failure) of the film or the substrate. The interfacial failure is not common since there is not a clearly defined interface, in other words, an interphase is a sort of mathematical plane or a sharp frontier with no thickness, while the interphase failure commonly happens since the interphase could be a single layer or a region. Finally, the cohesive failure is when the crack goes through the bulk film or substrate. As a rule of thumb, the adhesion is bad if the separation in the interface layer can be caused, while, if the separation occurs in the bulk, the adhesion is good. [20,23]

Among the different destructive techniques, the mostly used techniques are the fragmentation test, peel test, pull-off test, laser-spallation technique, buckling and delamination tests, superlayer test, indentation test, scratch test, and bending test.[19,63] In the following, the fragmentation tests will be discussed more in detail, in particular the uniaxial tensile testing, which is a universal test for mechanical characterization where the applied stress is uniform along the analysed sample, and compare this with other adhesion measurements.

3.4.1 Review of different destructive adhesion measurements

There are a lot of techniques for performing adhesion measurements, which will be briefly reviewed to make a comparison with the primary technique used for the present study. These are very simple techniques to carry out and the experimental data that can be extrapolated from these are straightforward. However, some limitations are outlined.

The indentation test is quite simple to carry out, in which it is possible to extrapolate from the measurement two primary information: hardness and elastic modulus. In order to perform this test, an indenter is needed, which must be harder than the coating (the tip of the indenter is usually made of diamond), then, this indenter presses the thin film in one point generating a local compressive stress. The most frequently used are Vickers and Knoop hardness tests, which depend on the geometry of the indenter.[3] From this test, it is also possible to extrapolate information about adhesion by introducing a stable crack into the interface between film and substrate, and the goal is to measure the resistance to crack propagation along the interface itself, but it is possible to carry out only for brittle thin film weakly bonded to the substrate.[19,63] One issue in performing this analysis is the substrate hardness, that is how deep is carried out this test, in fact deeper is performed the test, and higher is the influence of the mechanical properties of the substrate.[3,19]

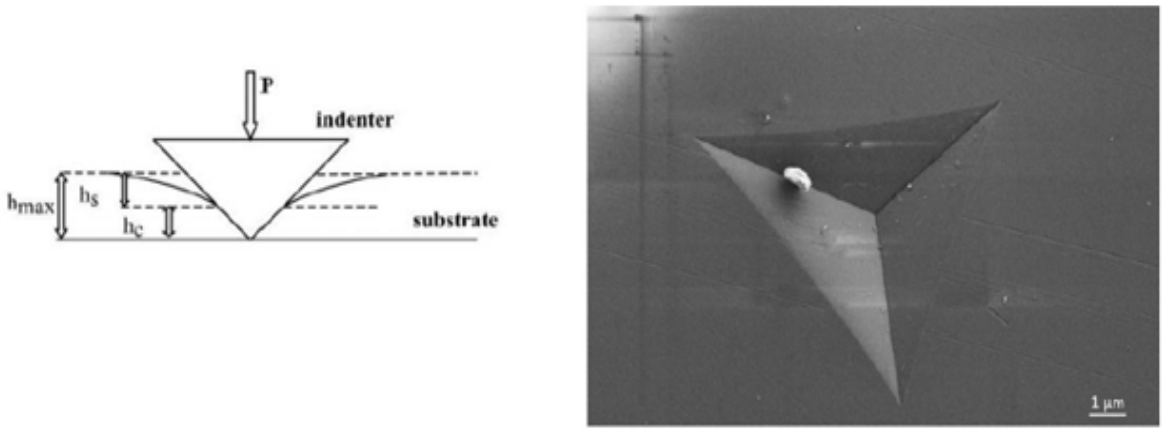

Figure 37 – a) Schematic representation of the indentation test apparatus[19] and b) an example of indentation test performed on alumina thin film[61]

Another technique for adhesion evaluation is the scratch test, in which a stylus with a certain radius tip is dragged along the coating so that above the layer surface there is a linear groove. The normal compressive load that is impressed from the stylus is increased in a stepwise or continuous manner, and the experimental test finishes when the film detaches from the substrate. From this, it is possible to extrapolate the critical load, which is then associated the fracture resistance of the interface.[19] There are several parameters that affect the critical load of thin film detachment, and they are summarized mainly in two categories: intrinsic parameters, such as loading rate, scratching speed, and indenter radius, and the extrinsic parameters, such as substrate and coating mechanical properties, friction force, and friction coefficient.[63] A SEM image of scratching test conducted on alumina thin film is reported in figure 38.[61]

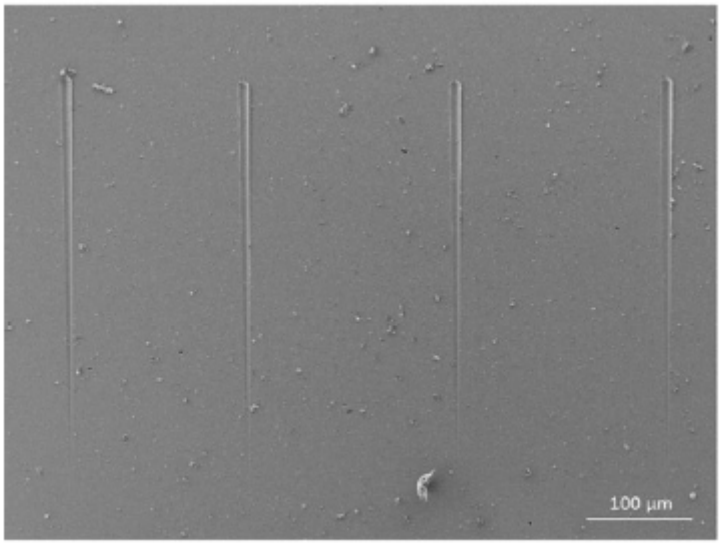

Figure 38 - SEM image of alumina coating surface in which scratching test has been conducted[61]

Finally, to complete this description of the main adhesion measurement techniques, the peel test and the pull-off test are worth mentioning two, which are used enough for measuring adhesion. Basically, the peel test consists of doing a coating strip using adhesive materials and detaching it from the substrate; thus, from this test, force needed to detach the layer from the substrate as a function of the angle is measured and the adhesion is measured when the angle is zero. Some considerations about this analysis are the importance of considering adhesives that

have a higher energy bonding with respect to the coating than the energy bonding between film and substrate and controlling the speed of peeling and the angle. A limitation of this test is when it is performed for very thin coatings, below 1 μm thickness. Instead, the pull-off test consists of a mechanical rod anchored to the coating with glue or similar, and under a critical applied load this rod detaches the film from the substrate. Some issues of this test are the compresence of tensile and shear forces due to erroneous alignment of the rod with the layer which create a different interpretation of the results[3,19], and the adhesive material used for anchoring the substrate to the rod must have an higher value of adhesive strength than of the interface.[64]

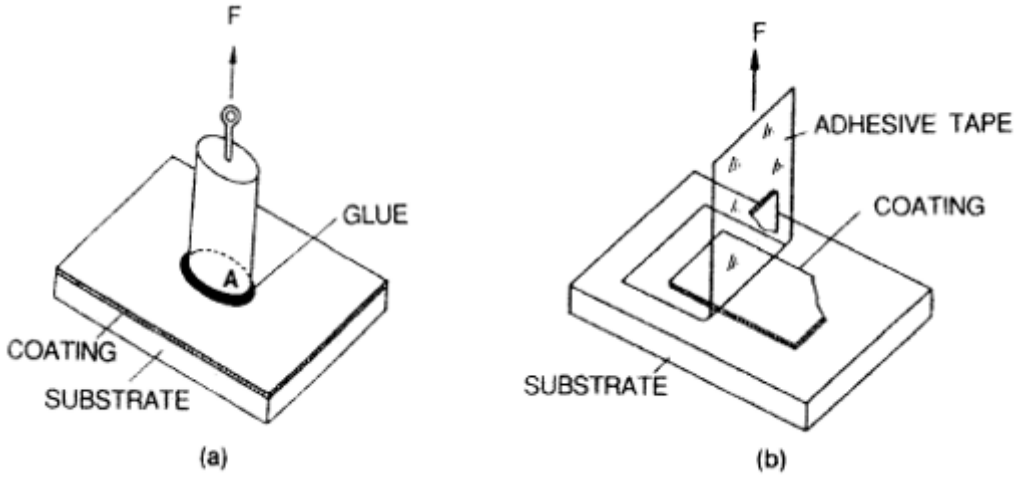

Figure 39 - Setup representations of the a) pull-off and b) peel test[3]

These experimental setups are easy to carry out, but their limitations imply values of adhesion measurements that are not easy to compare one to each other, although they provide acceptable values of adhesion. In order to perform a test with comparable results, there is a standard test that evaluates the formation of cracks into the coating under tensile stress. This technique is the fragmentation test which is analysed in detail in the next section.

3.4.2 Fragmentation test

Fragmentation measurements have a quite simple setup and well intuited data analyses, in which fundamentally the specimen is loaded in tension and the resulting damage is analysed as a function of strain, and sometimes the equipment is combined with imaging techniques like SEM, to in-situ observe the formation and the channelling propagation of cracks in the film. This measurement can be mainly summarized in three stages:

1) Crack onset and random cracking
2) Mid-point cracking (reduction in new cracks and initiation of transverse buckling
3) Delamination and crack saturation

The critical strain and toughness can be calculated from stage 1, while the adhesion parameters (like interfacial shear strength) can be calculated from stage 3.[19]

This mechanical test achieves good results if substrate is more brittle than coating, due to the fact that it is difficult to form channelling cracks inside the film if it has a higher value of elastic modulus with respect to the substrate, as demonstrated by Beuth relationship. A lot of works has been carried out in this sense and precise paralleling crack patterns have been observed. Agrawal et al. firstly tested 60 μm thickness of silica coating onto a ductile pure copper substrate, then, in another research, they tested again silica coating deposited onto copper and nickel substrates, where in the first case silica coating has 78 μm thickness, while in the second case, silica coating has 42 μm thickness.[50,51] Yang et al. instead have performed this mechanical test on a normal medium carbon steel dogbone over which it is deposited a thin film of 100 μm thickness brittle chromium.[64] Chen et al. presented their research on austenitic stainless steel dogbone as ductile substrate coated by 1.3 μm thickness of titanium nitride.[49] Finally, another example is given by an interlaboratory test consisting of measuring the adhesion of 5 μm thickness of chromium nitride onto austenitic stainless steel (AISI 304) coupons.[65]

These are few examples of researches which exploit the advantages of fragmentation test by uniaxial tensile strain, which is a well-known mechanical characterization of solid materials, previously described in the mechanical characterization of materials. In all these tests a common pattern can be obtained according to different parameters, such as the mechanical properties and material of coating and substrate, the critical loading at which first cracks appear and the

critical stress at which saturation of cracks is reached, the type of interface that is established, and the thickness of the coating. In all uniaxial tensile tests, the average crack spacing decreases rapidly reaching the saturation of cracks at a certain value of stress, while the crack opening (the width of the substrate exposure between two channelling cracks) increases.[66]

3.5 Experiment and results

In this section, a description of the experimental results is shown, thanks also to the collaboration with Polytechnic of Turin, which has carried out the measures under investigation. The experiment consists of depositing a thin alumina film by pulsed laser deposition (1 μm of thickness) onto polished AISI 316 dogbones, according to deposition parameters used for growing a compact and dense alumina coating. Then, these dogbones are uniaxially stretched and SEM images reveal the usual cracking pattern typical of brittle materials deposited onto ductile substrates.

3.5.1 Experimental procedures

Dogbones that were been coated are represented in the picture 40. These dogbones had a non-negligible surface roughness (dogbone A) since they are in a raw state, so that this roughness must be removed in order to favour a complete adherence of the coating on the substrate and avoiding delamination (dogbone B). A mechanical polishing was necessary, and, to do this, a lapping machine was used. Using different silicon carbide discs with a gradually smaller particle size and aqueous solutions with dispersion of diamond particles, it was possible to obtain a fairly low roughness, after which the lapped surface had to be cleaned. A further cleaning of various residues and impurities on the surface was done by sonication in acetone for 15 minutes.

Setup of the deposition parameters such as target to substrate distance, rotation and translation of the substrate to be coated, oxygen partial pressure in the chamber, and laser parameters has been performed using pieces of pure silicon taken from wafer, which are coated by a very thin film of alumina (few nanometers of thickness). Thickness of the coating has been measured using profilometer and the value obtained is used to quantify the number of laser pulses useful to reach more or less 1 μm thickness of alumina on stainless steel dogbone. The compactness of the coating has been visualized by SEM images.

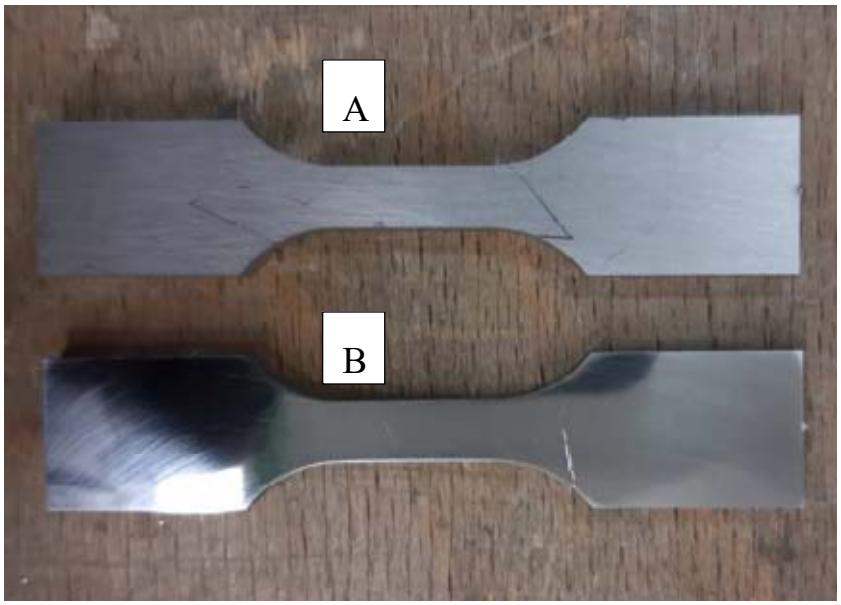

Figure 40 - Uncoated AISI 316 dogbones before (A) and after (B) mechanical polishing

Once the setup was completed, deposition on dogbones has been carried out putting a couple of them at a time into the chamber; then, before deposition, another cleaning treatment of argon ions was performed. The deposition time required for depositing 1 μm thickness of alumina was about 8/10 hours per two dogbones. The result is shown in the picture 41, in which interference fringes are clearly visible. Finally, these alumina-coated dogbones were uniaxially pulled in tension and analysed by SEM at Polytechnic of Turin.

Figure 41 - Alumina-coated AISI 316 dogbone

3.5.2 Results and discussion of thin film fracture toughness

In the following, geometrical and mechanical parameters of AISI 316 dogbones are listed (the subscript s stands for substrate):

- Thickness $H = 4\ mm$
- Lowest value of width (taken in the middle of the dogbone) $W = 6\ mm$
- Lowest value of cross section $A = 24\ mm^2$
- Young modulus $E_s = 190\ GPa$
- Poisson ratio $\nu_s = 0.3$[28]
- Yield strength $\sigma_s = 400\ MPa$
- Ultimate tensile strength $\sigma_{s,uts} = 640\ MPa$

According to SEM images in the picture 42, first cracks appear at more or less 7 kN, which means that the stress acting on the middle of the dogbone σ_0, where it is found the lowest value of cross section A, is

$$\sigma_{s,0} = \frac{F}{A} = 292\ MPa$$

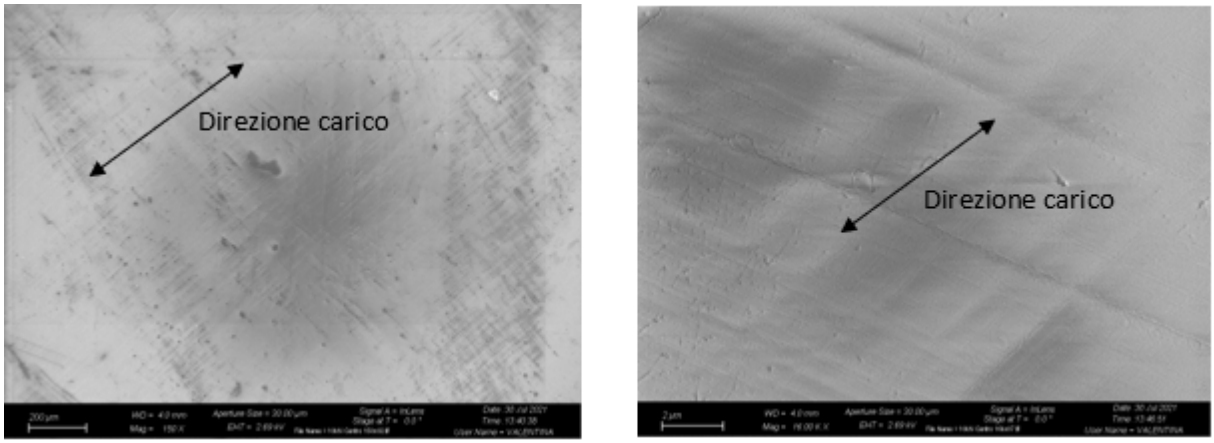

Figura 42 - SEM images of alumina surface after a loading of 7 kN

This value, maybe the onset of the first cracks, is well below the yield strength of the substrate, so, in the first approximation, no plastic deformation of the substrate induces cracks into the film. Assuming perfect adhesion between film and substrate, strain acting on the substrate induces the same strain on the coating:

$$\varepsilon_{s,0} = \frac{\sigma_0}{E_s} = 1.54 * 10^{-3} = 0.154\% = \varepsilon_{f,0}$$

The stress acting on the middle of the coating is:

$$\sigma_{f,0} = E_f \varepsilon_{f,0} = 300\ MPa$$

Where $E_f = 195\ GPa$ is taken from Ferrè et al.[61] This value of stress is considered constant along the coating cross section taken in the middle of the dogbone, according to the hypothesis of thin film, highlighted in section 2.4.2.

Now, an evaluation of the fracture resistance Γ_f and the stress intensity factor $K_{f,IC}$ of the alumina coating can be done by recalling the Beuth formulation, under the hypothesis of linear elastic materials:

$$\Gamma_f = G_{SS} = \frac{\pi \sigma_{f,0}^2 h_f}{2\bar{E}_f} g(\alpha, \beta)$$

The reduced elastic moduli for film ($\nu_f = 0{,}294$) and substrate ($\nu_s = 0.3$):

$$\bar{E}_f = \frac{E_f}{1 - \nu_f^2} = 213.4\ GPa$$

$$\bar{E}_s = \frac{E_s}{1 - \nu_s^2} = 208.8\ GPa$$

The non-dimensional parameter $g(\alpha, \beta)$ can be extrapolated from plots in the literature, or some empirical formulations, for example, taken from Yin et al.:[48]

$$g(\alpha, \beta) = \frac{1.258 - 0.4\alpha - 0.26\alpha^3 - 0.3\alpha^4}{1 - \alpha} = 1.267$$

Where $\alpha = (\bar{E}_f - \bar{E}_s)/(\bar{E}_f + \bar{E}_s) = 0.0109$ (β is considered in this formulation negligible).

Substituting the values of $\bar{E}_f$ and $g(\alpha, \beta)$ into the equation for Γ_f, and taking $h_f = 1\ \mu m$, we get $\Gamma_f = 0.84\ J/m^2$, while, by using the Irwin's relation, the stress intensity factor should be

$$K_{f,IC} = \sqrt{\Gamma_f \bar{E}_f} = 0.42\ MPa\sqrt{m}$$

As it stated in the previous chapter, these two values are considered independent on the geometry of the film and substrate, and the applied stress, they only depend on the material, however, these values are one order of magnitude less than specific values for ceramic materials. Small values of fracture toughness correspond in general to a brittle behaviour, in fact, if they are fixed the values of the dimensionless fracture toughness $g(\alpha, \beta)$, and the thickness and the reduced elastic modulus of the of the film, h_f and $\bar{E}_f$, respectively, then, lower is the value of the fracture toughness, lower is the value of the fracture stress $\sigma_{f,0}$ at which channelling cracks can propagate. By this fact, alumina coating seems to have a more brittle

behaviour with respect to the bulk alumina, where its stress intensity factor is in the range of 4.1 to 5.9 $MPa\sqrt{m}$. For a deeper analysis, once it is fixed the materials under studies, thus fixing the film elastic modulus and the dimensionless parameter $g(\alpha, \beta)$, it could be interesting to evaluate the fracture toughness for different alumina thicknesses, and, if the Beuth relationship is valid, then a decreasing of the coating thickness corresponds to an increasing of the fracture stress $\sigma_{f,0}$.

3.5.3 Results and discussion of the interfacial shear strength

During the uniaxial tensile stress, the intrinsic pattern of parallel cracks can be noticed according to the theory of multiple crack propagation, and more specifically this can be seen at 8 kN of external loading, as depicted in figure 43a. Associated with this first crack pattern, small pieces of the coating detach from the substrate. Looking at picture 43b, the increase in the applied load corresponds to more pronounced detaching areas of the coating from the substrate, and a decreasing in the spacing between channelling cracks. An approximated evaluation of the crack spacing by analysing the SEM images provides 100 μm and 50 μm, respectively. Of course, these values must be accurately evaluated by looking several images and realizing a statistical distribution of different crack spacing sizes.

According to Chen et al., they supposed four stages that are consecutive with applied stress increase for the formation of a set of parallel cracks, which are summarized in a plot crack density vs. strain percentage. These stages are multiplication, in which cracks density increase rapidly, stabilization, where the crack density reaches a saturation value, cross-linking, where 45°-tilted cracks with respect to the crack pattern can be formed, and spallation, where pieces or large areas of coating detach from the substrate. They supposed that cross-linking stage can appear due to the necking of the substrate. For the spallation, they supposed that a rougher substrate is the main responsible for the local detachment, which is also consistent with the theory described in section 2.2.2, and this roughness can be provoked not only with lower polishing of the surface sample, but also by the applied stress.[67]

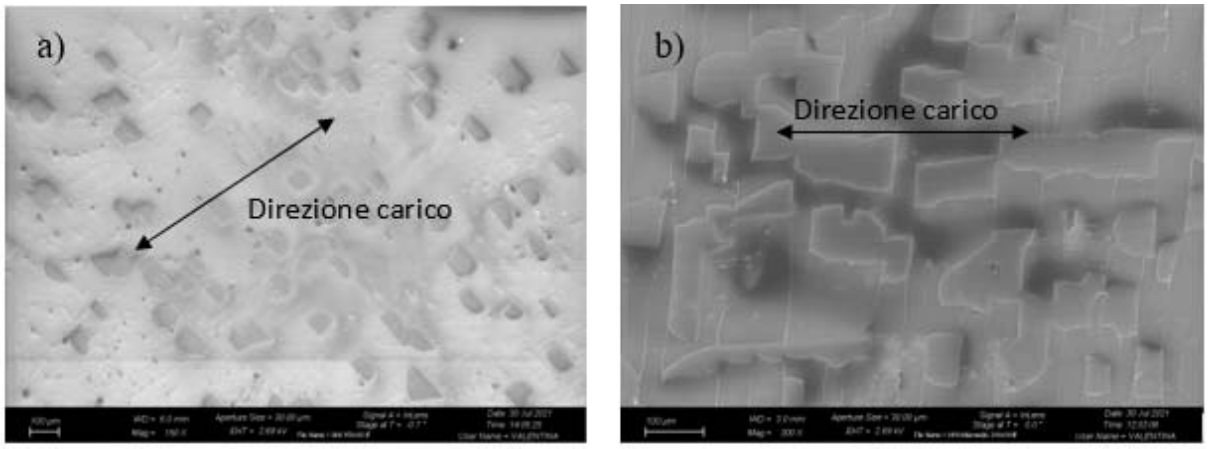

Figura 43 – Alumina crack patterns in the middle of the sample at a) 8 kN and b) 9 kN

By looking the SEM images of alumina in figure 43, we can notice that no tilted cracks have been formed, and this is in accordance with the experimental results, in fact, the applied stresses at 8 kN and 9 kN are again below the yield strength of the substrate, so no plastic deformation are involved in the formation of tilted cracks; however, detachment is present. Since plastic deformation of the substrate is one of the main issues for detachment, which, however, is not happened, thus, spallation can be explained with other two reasons: the former, which is more probable, is related to the roughness of the substrate, which has to be even lower than it was realized for these samples, while the second reason is related to a poor bonding strength between alumina coating and stainless steel substrate.

Finally, an evaluation of the interfacial shear strength is not easy to be done in the present study, because of lack of SEM images which allow to better understand and visualization of the crack density, making a statistical distribution, and their spacing between them.

3.6 Conclusion and outlook

Several techniques for measuring quantities related to the mechanical properties and adhesion of thin films onto substrates can be found in literature, but the one that has a future perspective is that to test a film/substrate system pulling it uniaxially in tension. Hence, parallel channelling cracks are formed in a regular array forming a pattern, perpendicular to the applied stress. By in-situ observation, this test can correlate the appearance of random cracks to the external load (it is more convenient to evaluate the strain induced by the applied stress, since the same strain is applied both for the coating and the substrate).

The major advantage of this test instead of other is related to the application of tensile testing for different combination of film/substrate systems by the evaluation of the crack formation into the coating. Using the theory derived by Hutchinson[26] and Beuth[35] in their works, respectively, fracture toughness of the film can be evaluated, and different models can be used to analyse the crack pattern formation and the related interfacial shear strength. For a better analysis different coating thickness could be evaluated in order to interpolate the results, however, analytical models based on energetic balance could not be enough for an extensive results, so an implementation of this study could be done by using computational models based on finite element analysis programs.

Bibliography

1. Moorthy SBK. *Thin film structures in energy applications.* Springer; 2015.

2. Ferré FG, Ormellese M, Di Fonzo F, Beghi M. Advanced Al2O3 coatings for high temperature operation of steels in heavy liquid metals: A preliminary study. *Corros Sci*. 2013;77:375-378.

3. Ohring M. *Materials science of thin films.* Elsevier; 2001.

4. Greene JE. Tracing the 5000-year recorded history of inorganic thin films from ∼3000 BC to the early 1900s AD. *Applied Physics Reviews*. 2014;1(4):041302.

5. Pedeferri P, Ormellese M. *Corrosion science and engineering.* Springer; 2018.

6. Morosanu CE. *Thin films by chemical vapour deposition.* Vol 7. Elsevier; 2016.

7. Eason R. *Pulsed laser deposition of thin films: Applications-led growth of functional materials.* John Wiley & Sons; 2007.

8. Lorenz M. Pulsed laser deposition. *digital Encyclopedia of Applied Physics*. 2019:1-29.

9. Stafe M, Marcu A, Puscas NN. *Pulsed laser ablation of solids: Basics, theory and applications.* Vol 53. Springer Science & Business Media; 2013.

10. GARCIA FERRE F. Radiation tolerant nanoceramic coatings for lead fast reactor nuclear fuel cladding. . 2014.

11. Mihailescu IN, Caricato AP. Pulsed laser ablation: Advances and applications in nanoparticles and nanostructuring thin films. . 2018.

12. Rijnders G, Blank DH. Growth kinetics during pulsed laser deposition. *Pulsed Laser Deposition of Thin Films*. 2007:177-190.

13. Guenther KH. Revisiting structure zone models for thin film growth. . 1990;1324:2-12.

14. Braun S, Foltyn T, van Loyen L, Moss M, Leson A. Multi component EUV multilayer mirrors. . 2003;5037:274-285.

15. Bottiger J, Chevallier J, Kringhoj K, Schweitz K. Stresses in thin films. *Adhesion Aspects of Thin Films*. 2001;1:1-16.

16. CAMMARATA RC. Surface effects on intrinsic thin-film stresses. *Adhesion Aspects of Thin Films, volume 2*. 2005;2:3.

17. Thurner G, Abermann R. Internal stress and structure of ultrahigh vacuum evaporated chromium and iron films and their dependence on substrate temperature and oxygen partial pressure during deposition. *Thin Solid Films*. 1990;192(2):277-285. doi: https://doi.org/10.1016/0040-6090(90)90072-L.

18. Haque M, Saif M. In-situ tensile testing of nano-scale specimens in SEM and TEM. *Exp Mech*. 2002;42(1):123-128.

19. Gunda M, Kumar P, Katiyar M. Review of mechanical characterization techniques for thin films used in flexible electronics. . 2017;42(2):129-152.

20. Pulker HK, Perry AJ, Berger R. Adhesion. *Surface Technology*. 1981;14(1):25-39. doi: https://doi.org/10.1016/0376-4583(81)90005-4.

21. Pulker HK. Chapter 5 - glass and thin films. . 1999:73-102. doi: https://doi.org/10.1016/B978-044450103-5/50008-X.

22. Mattox D. *Interface formation and the adhesion of deposited thin films.* Vol 65. Technical Information Division, Sandia Corporation; 1965.

23. Mittal K. Adhesion measurement of films and coatings: A commentary. *Adhesion measurement of films and coatings*. 1995;1.

24. Brown SD. Adherence* failure and measurement: Some troubling questions. *J Adhes Sci Technol*. 1994;8(6):687-711.

25. Hutchinson JW. Stresses and failure modes in thin films and multilayers. *Notes for a Dcamm Course.Technical University of Denmark, Lyngby*. 1996;1:14.

26. Hutchinson JW, Suo Z. Mixed mode cracking in layered materials. *Adv Appl Mech*. 1991;29:63-191. doi: https://doi.org/10.1016/S0065-2156(08)70164-9.

27. Mei H, Pang Y, Im SH, Huang R. Fracture, delamination, and buckling of elastic thin films on compliant substrates. . 2008:762-769.

28. Callister Jr WD, Rethwisch DG. *Callister's materials science and engineering.* John Wiley & Sons; 2020.

29. Wikipedia. Stress-strain curve. https://en.wikipedia.org/wiki/Stress-strain_curve. Updated 2022.

30. Dieter, George Ellwood.,Bacon, David.,. *Mechanical metallurgy.* London: McGraw-Hill Book; 1988.

31. Vergani L. *Meccanica dei materiali / laura vergani.* Milano etc.: Milano etc. : McGraw-Hill; 2001.

32. Thouless MD. Cracking and delamination of coatings. *Journal of Vacuum Science & Technology A: Vacuum, Surfaces, and Films*. 1991;9(4):2510-2515.

33. Dundurs J. Effect of elastic constants on stress in A composite under plane deformation. *J Composite Mater*. 1967;1(3):310-322.

34. Dundurs J. Discussion:"Edge-bonded dissimilar orthogonal elastic wedges under normal and shear loading"(bogy, DB, 1968, ASME J. appl. mech., 35, pp. 460–466). . 1969.

35. Beuth JL. Cracking of thin bonded films in residual tension. *Int J Solids Structures*. 1992;29(13):1657-1675. doi: https://doi.org/10.1016/0020-7683(92)90015-L.

36. Hutchinson JW. Mixed mode fracture mechanics of interfaces. *Metal-ceramic interfaces*. 1990;1990:295-306.

37. Suga T, Elssner G, Schmauder S. Composite parameters and mechanical compatibility of material joints. *J Composite Mater*. 1988;22(10):917-934.

38. Volinsky A, Moody N, Gerberich W. Interfacial toughness measurements for thin films on substrates. *Acta materialia*. 2002;50(3):441-466.

39. Evans A, Rühle M, Dalgleish B, Charalambides P. The fracture energy of bimaterial interfaces. *Metallurgical Transactions A*. 1990;21(9):2419-2429.

40. Evans AG, Hutchinson JW. Effects of non-planarity on the mixed mode fracture resistance of bimaterial interfaces. *Acta Metallurgica*. 1989;37(3):909-916.

41. Ye T, Suo Z, Evans A. Thin film cracking and the roles of substrate and interface. *Int J Solids Structures*. 1992;29(21):2639-2648.

42. Zak A, Williams ML. Crack point stress singularities at a bi-material interface. . 1962.

43. Nakamura T, Kamath SM. Three-dimensional effects in thin film fracture mechanics. *Mech Mater*. 1992;13(1):67-77.

44. Ambrico JM, Begley MR. The role of initial flaw size, elastic compliance and plasticity in channel cracking of thin films. *Thin Solid Films*. 2002;419(1-2):144-153.

45. Hu M, Evans A. The cracking and decohesion of thin films on ductile substrates. *Acta Metallurgica*. 1989;37(3):917-925.

46. Beuth J, Klingbeil N. Cracking of thin films bonded to elastic-plastic substrates. *J Mech Phys Solids*. 1996;44(9):1411-1428.

47. Xia ZC, Hutchinson JW. Crack patterns in thin films. *J Mech Phys Solids*. 2000;48(6-7):1107-1131.

48. Yin H, Paulino G, Buttlar W. An explicit elastic solution for a brittle film with periodic cracks. *Int J Fract*. 2008;153(1):39-52.

49. Chen BF, Hwang J, Chen IF, Yu GP, Huang J-. A tensile-film-cracking model for evaluating interfacial shear strength of elastic film on ductile substrate. *Surface and Coatings Technology*. 2000;126(2):91-95. doi: https://doi.org/10.1016/S0257-8972(99)00669-6.

50. Agrawal DC, Raj R. Measurement of the ultimate shear strength of a metal-ceramic interface. *Acta Metallurgica*. 1989;37(4):1265-1270. doi: https://doi.org/10.1016/0001-6160(89)90120-X.

51. Agrawal DC, Raj R. Ultimate shear strengths of copper-silica and nickel-silica interfaces. *Materials Science and Engineering: A*. 1990;126(1-2):125-131.

52. Wang K, Zhang F, Bordia RK. FEM modeling of in-plane stress distribution in thick brittle coatings/films on ductile substrates subjected to tensile stress to determine interfacial strength. *Materials*. 2018;11(4):497.

53. Anderoglu O, Marino A, Hosemann P. Corrosion in heavy liquid metals for energy systems. *JOM*. 2021;73(12):3998-3999.

54. Gorynin I, Karzov G, Markov V, Yakovlev V. Structural materials for atomic reactors with liquid metal heat-transfer agents in the form of lead or lead—Bismuth alloy. *Metal Science and Heat Treatment*. 1999;41(9):384-388.

55. Levin I, Brandon D. Metastable alumina polymorphs: Crystal structures and transition sequences. *J Am Ceram Soc*. 1998;81(8):1995-2012.

56. Auerkari P. *Mechanical and physical properties of engineering alumina ceramics.* Vol 23. Technical Research Centre of Finland Espoo; 1996.

57. Gitzen WH. *Alumina as a ceramic material.* Wiley; 1970.

58. Andersson JM. *Controlling the formation and stability of alumina phases*. 2005.

59. Holmberg K, Matthews A. Chapter 4 tribological properties of coatings. *Tribology Series*. 1994;28:125-256. doi: https://doi.org/10.1016/S0167-8922(08)70754-5.

60. Di Fonzo F, Tonini D, Li Bassi A, et al. Growth regimes in pulsed laser deposition of aluminum oxide films. *Appl Phys A*. 2008;93(3):765-769.

61. García Ferré F, Bertarelli E, Chiodoni A, et al. The mechanical properties of a nanocrystalline Al2O3/a-Al2O3 composite coating measured by nanoindentation and brillouin spectroscopy. *Acta Materialia*. 2013;61(7):2662-2670. doi: https://doi.org/10.1016/j.actamat.2013.01.050.

62. Frankberg EJ, Kalikka J, García Ferré F, et al. Highly ductile amorphous oxide at room temperature and high strain rate. *Science*. 2019;366(6467):864-869.

63. Chalker P, Bull S, Rickerby D. A review of the methods for the evaluation of coating-substrate adhesion. *Materials Science and Engineering: A*. 1991;140:583-592.

64. Yang BQ, Chen GN, Chen XJ. Uniaxial tensile and cross-sectional indentation tests to investigate the adhesion between the brittle cr coating and the ductile steel substrate. . 2011;52:854-858.

65. Aldrich SG, Jennet NM, Houdsen J. A round robin to measure the adhesion of thin coatings. . 2004;NPL Report. DEPC-MPE 001.

66. Xie C, Tong W. Cracking and decohesion of a thin Al2O3 film on a ductile Al–5%Mg substrate. *Acta Materialia*. 2005;53(2):477-485. doi: https://doi.org/10.1016/j.actamat.2004.10.005.

67. Chen BF, Hwang J, Yu GP, Huang JH. In situ observation of the cracking behavior of TiN coating on 304 stainless steel subjected to tensile strain. *Thin Solid Films*. 1999;352(1):173-178. doi: https://doi.org/10.1016/S0040-6090(99)00342-9.